GIFT 핵연료 코드개발 현황 및 이미지 분석법을 활용한 지르코늄 피복관 수소취화 현상 연구

서울대학교 원자핵공학과

이유호, 심규석, 노현택, 김진수, 김동주, 우다현, 김동욱, 이찬수

leeyouho@snu.ac.kr

2022 추계 원자력학회
계산과학/AI 활용 핵연료 및 원자력 재료연구 워크샵
2022.10.19

1. Development of GIFT

코드 개발 배경

- **국산 핵연료 안전/성능 해석 코드의 부재**
  - 우리나라는 U.S NRC의 안전규제 코드인 FRAPCON/FRAPTRAN을 연구와 안전규제 용도로 사용해 왔음.
  - 국산화 된 코드를 활용하는 원자로 물리 및 열수력 분야와 비교할 때 큰 차이가 있음.
  - 산업체 (한전원자력연료)가 개발한 사업자용 코드가 있으나, 이는 비공개 코드로 연구 목적으로 사용될 수 없음.

- **급변하는 국제 핵연료 코드 공개 범위**
  - 미국은 FRAPCON/FRAPTRAN의 개발을 중단 하였으며 이를 대체할 FAST 코드의 소스 코드는 공개하지 않는 것을 방침으로 함.
  - INL에서 연구목적으로 개발된 FEM 기반 코드인 BISON을 국내 연구진이 활용하기에는 상당한 제약이 있고 지속 가능하지 않음.

- **핵연료 전산 모사의 새로운 모델개발 필요성 대두**
  - 우리나라 핵연료개발의 주요 현안으로 대두된 (1) 사고저항성핵연료 (2) 건식저장거동 (3) i-SMR 핵연료 (4) 고연소도 핵연료 현안을 다룰 수 있는 자체적 핵연료 코드 필요

GIFT 코드 목표 성능

GIFT 코드개발 (written in C++)

고심도 ATF 모사 및 미래 원자력 를 위한 추가 모델 성능 정리

(흰색) : 현행 체계 모델 적용가능 (녹색) : GIFT 특화 모델

	FRAPCON-4.0/FRAPTRAN-2.0	GIFT
소결체 거동 모델	UO_2 소결체	UO_2 소결체
피복관 구조해석 모델 충실도	1D 모델 (Thin-wall approximation)	2차원 축대칭 모델 도입
다층 피복관 구조 해석 모델	반영 안됨	코팅피복관, SiC 피복관 모사
소결체-피복관 기계적 상호작용 (PCMI)	Rigid Pellet Model	Rigid Pellet Model
축방향 피복관 조사성장 구조해석	반영 안됨	반영 필요
피복관 벌루닝 및 파열	ATF 코팅영향 미반영	ATF 코팅영향 반영필요
산화모델	실험상관식 기반 단순모델. 코팅 미반영.	고심도 해석모델. Zr-Cr-O 거동모델 개발.
건식저장 사용후 핵연료 모델	제한적	확장 모사
수소 확산 모델	반영 안됨	모사
가돌리니아 삽입 모델	반영 안됨	i-SMR 적용 관점에서 모사

Code Development

- **GIFT, Fuel performance code for steady-state**
  - Language: C++ 14
  - Material Property Library: MATPRO 1.16
  - Matrix Calculation Library: Eigen 3.4.1-rc

```cpp
#include "calcoolT.h"      You, 3개월 전 • 초기 커밋. …

/// @brief this function calculates bulk coolant temperatures of each axial mesh and other related properties.
///
/// @param namax # of axial meshes
/// @param ntmax # of time steps
/// @param dco cladding outer diameter                                 [m]
/// @param delh length of axial meshes                                 [m]
/// @param pitch center-to-center distance between rods in a square array  [m]
/// @param tw coolant inlet temperature                                [K]
/// @param g coolant mass flux                                         [kg/m2/s]
/// @param p2 coolant pressure                                         [psi]
/// @param B linear power of the axial mesh                            [W/m]
/// @param spent_dry order of time step when dry storage begins
/// @param rhof_old old value of unsaturated bulk coolant density      [lbm/ft3]
/// @param time time index, which is equal to (present step order - 1)
///
/// @return coolT1 bulk coolant temperature of each axial meshes       [K]
/// @return linpower linear power of each axial meshes                 [W/m]
/// @return qc surface heat flux w/o oxide thickness                   [W/m2]
/// @return rhof unsaturated bulk coolant density                      [lbm/ft3]
/// @return coolTtop bulk coolant temperature at the top of fuel pellet  [K]
/// @return deh effective hydraulic diameter at the top axial mesh     [ft]

CALCOOLT calcoolT(SettingNums* SetupNums, double* dco, double* delh, double pitch, double tw, double g, double p2, double* B, double* rhof_old, int time) {

    int namax = SetupNums->AxialIndexNum;
    int ntmax = SetupNums->TimeIndexNum;
    int spent_dry = SetupNums->DryStorageTimeIndexNum;

    CALCOOLT value;
    value.coolT1 = (double*)calloc(namax, sizeof(double));
    value.linpower = (double*)calloc(namax, sizeof(double));
    value.qc = (double*)calloc(namax, sizeof(double));
    value.rhof = (double*)calloc(namax, sizeof(double));
    value.deh = (double*)calloc(namax, sizeof(double));
    value.coolTtop = 0;

```

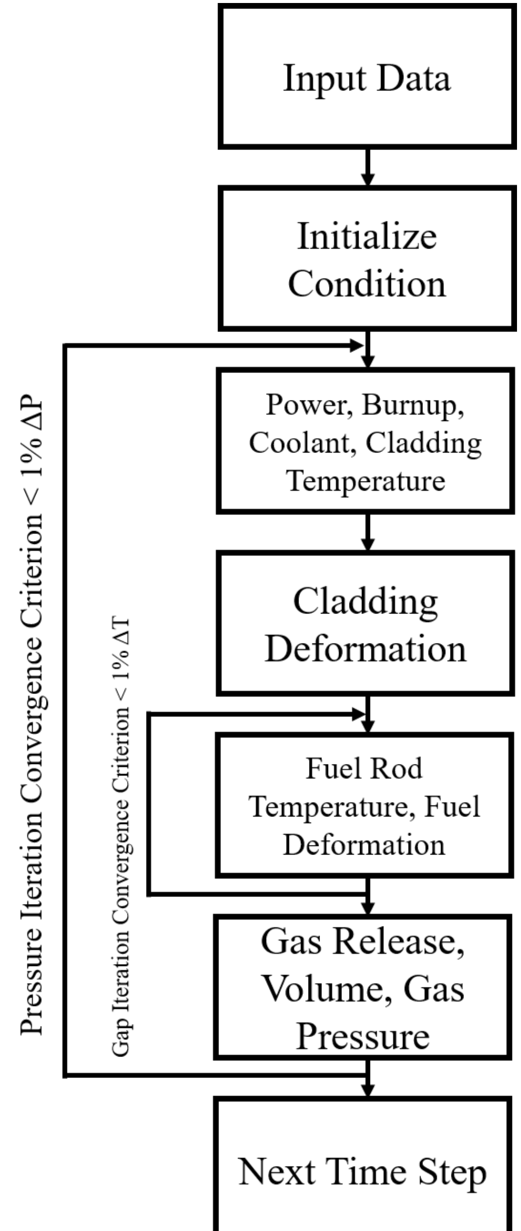

Code Structure (total ~100 individual subroutines)

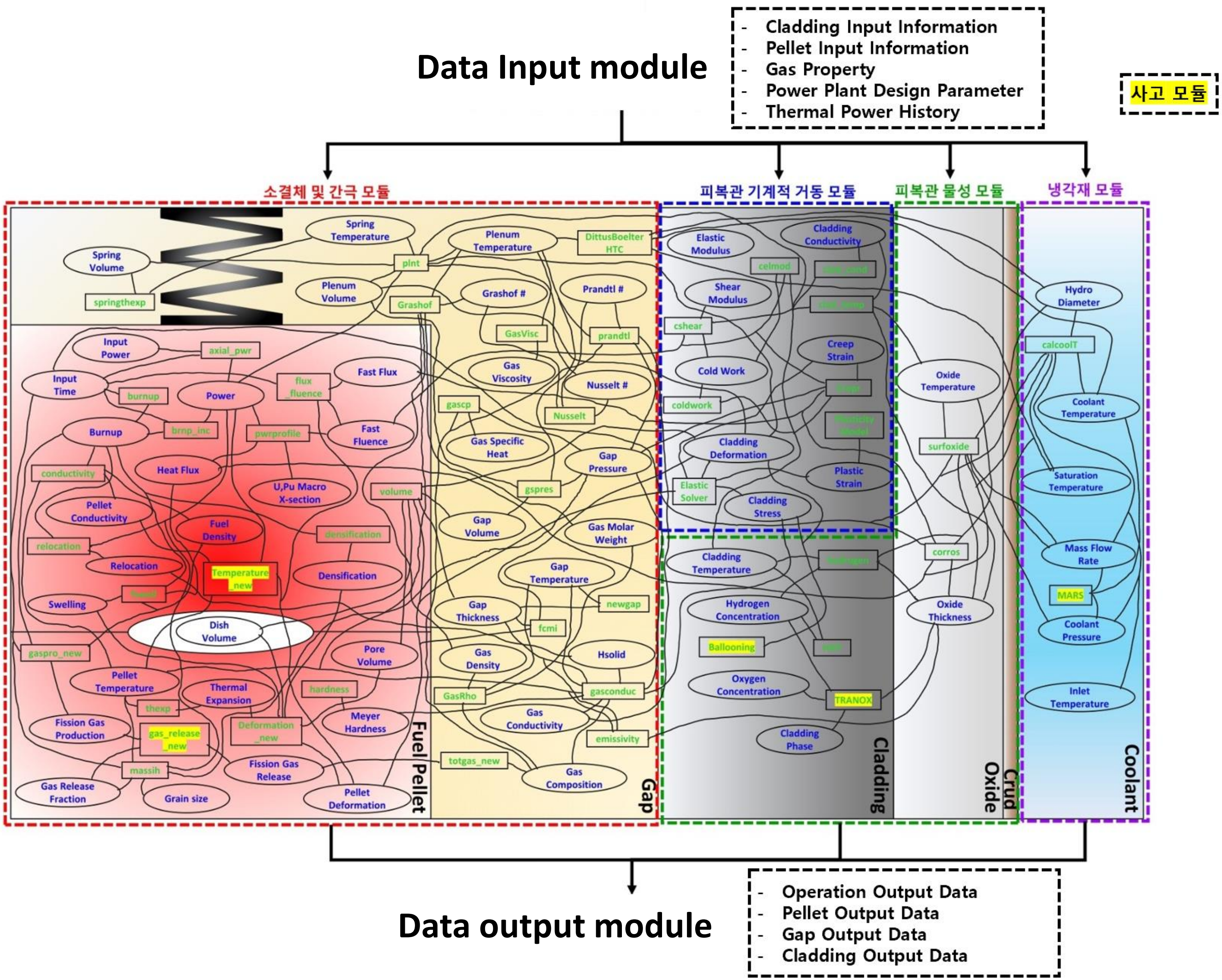

Cladding mechanical model development

- **2D axis-symmetric cladding mechanical model**
  - FDM method used
  - Multi-layer model
  - Full-length calculation
  - More accurate than 1D model(thin-wall approximation)
  - Faster than FEM methods

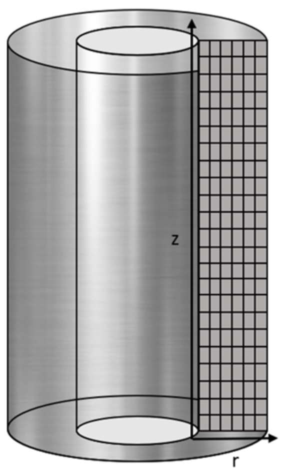

2D (axis-symmetric) full length fuel rod

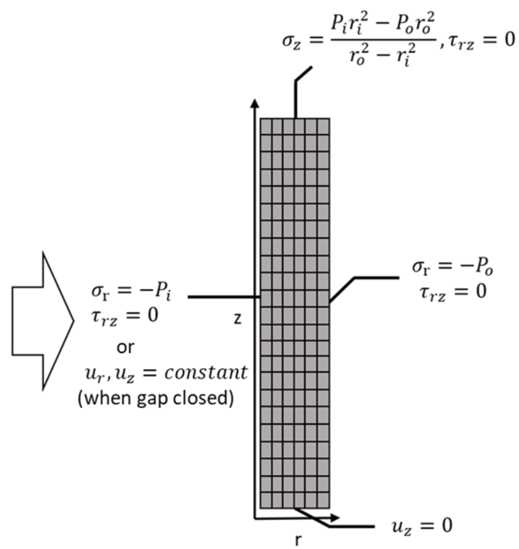

Boundary conditions

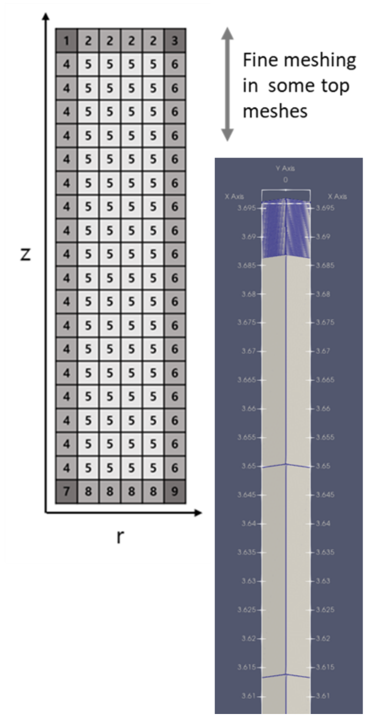

Cladding plasticity

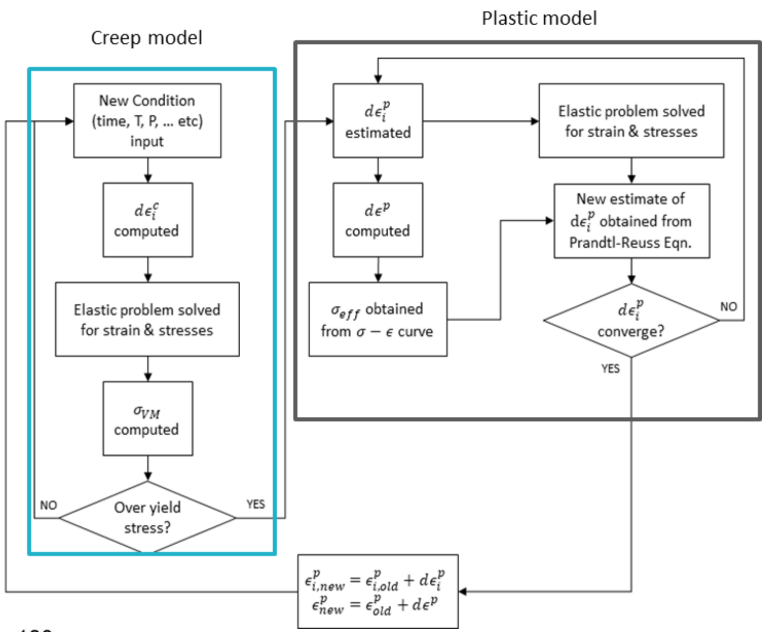

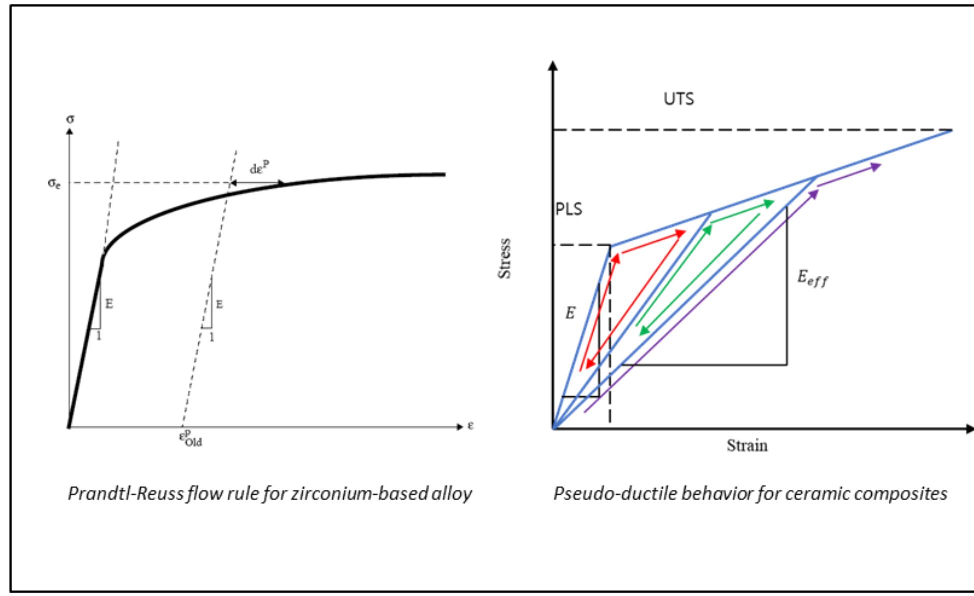

Material-dependent plasticity model

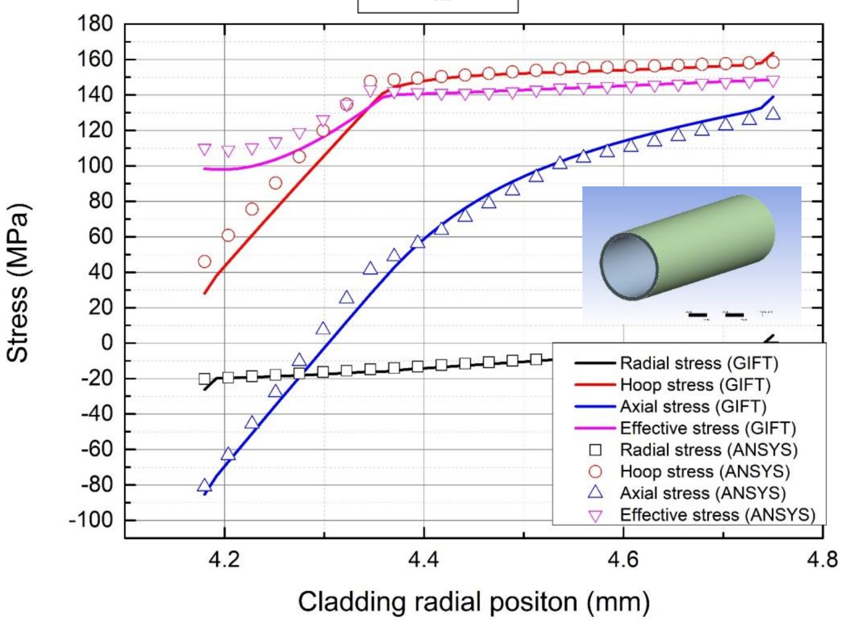

<ANSYS와의 소성이 고려된 구조해석 결과 비교 검증>

- Plasticity model enabled and verified against commercial FEM codes.
- Plastic behavior of the coating layer can be modeled by using a stress-strain curve of the coating.
- Pseudo-ductile behavior of the SiC/SiC_f composite is modeled.

Pellet-Cladding Mechanical Interaction(PCMI) model

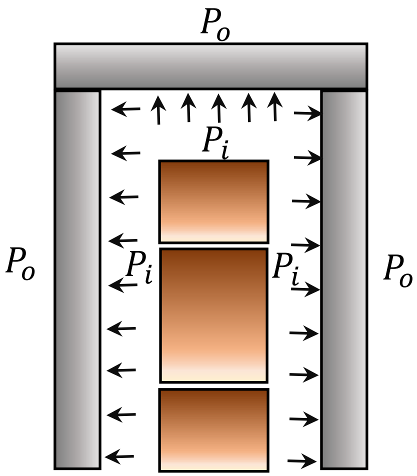

Open gap

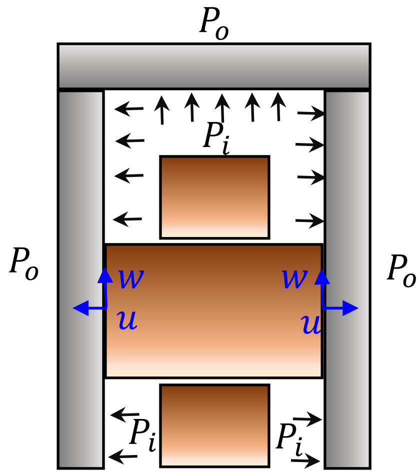

closed gap

$$A\vec{x} = \vec{b}$$

Discretization scheme & inter-node interaction

Boundary conditions

Matrix and B.C conditioning for every different pellet-cladding interaction state in the fuel rod

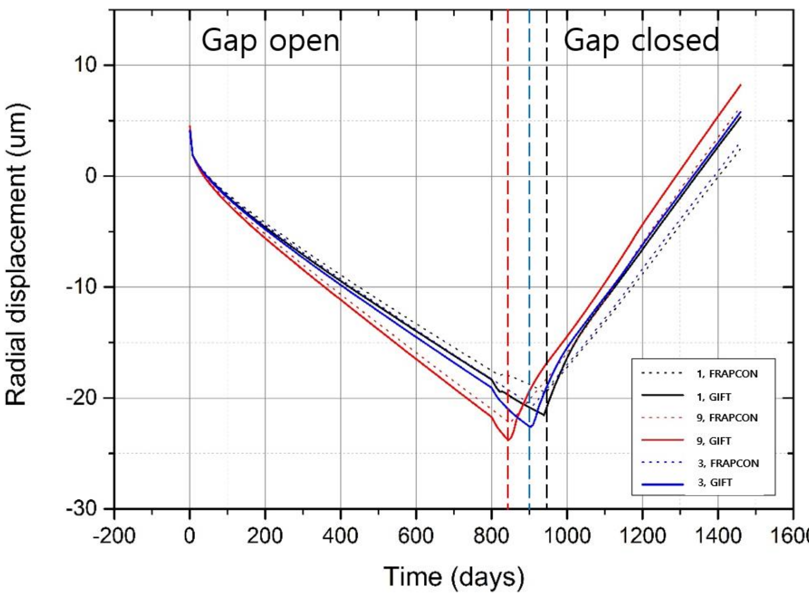

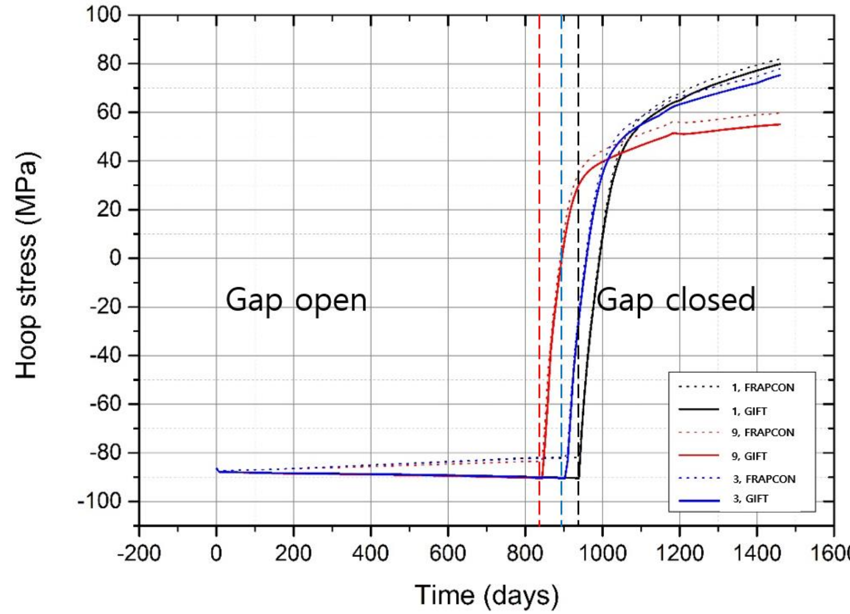

<Cladding performance comparison with FRAPCON>

GIFT 구조해석 모듈 검증 결과

- **피복관 크립문제를 GIFT로 해석하여 FEA 결과와 비교**

  - FEA를 참조해 (Reference solution)로 하여 코드 검증

<일반 피복관>

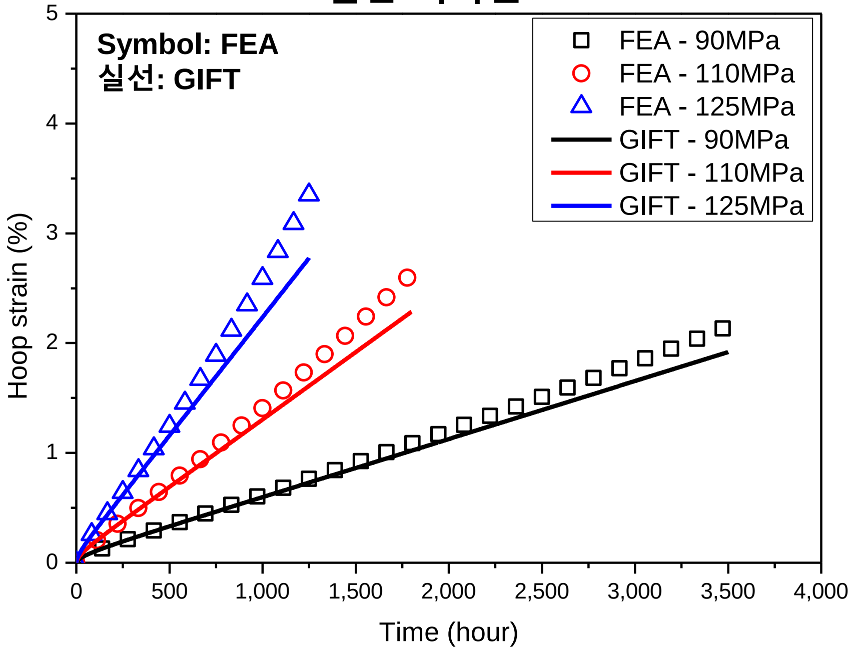

<코팅 피복관>

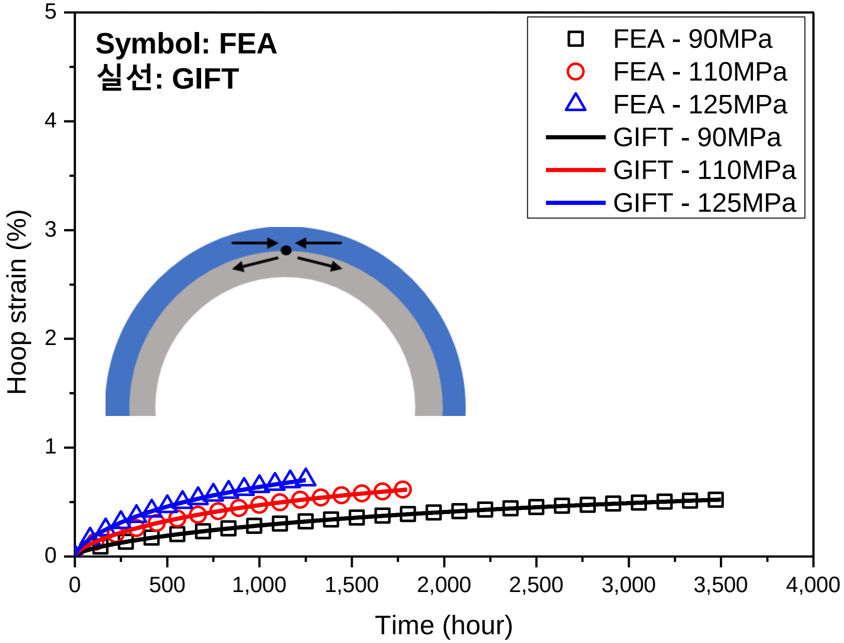

- **검증 결과**

  - <u>코팅 피복관의 감소된 크립 변형률 예측 가능 (as well as excellent agreement with FEA)</u>

  - 일반 피복관의 변형 예측 정확도 ↓ (변형률 1% 이상에서부터 오차 증가)

  - GIFT 구조해석 모듈: 미소 변형 기반 → 대변형 영역에서 오차 발생

  - 대변형 영역 해석 정확도 향상을 위한 formulation 및 코드 수정 진행 中

코팅 피복관 크립 실험 결과

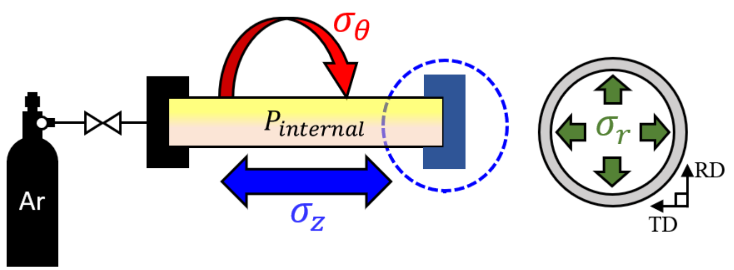

- Cladding tube creep tests with internal pressurization at Korean Nuclear Fuel (KNF)
- Coating thickness: 16.8 μm
- Base material: Zr-Nb cladding

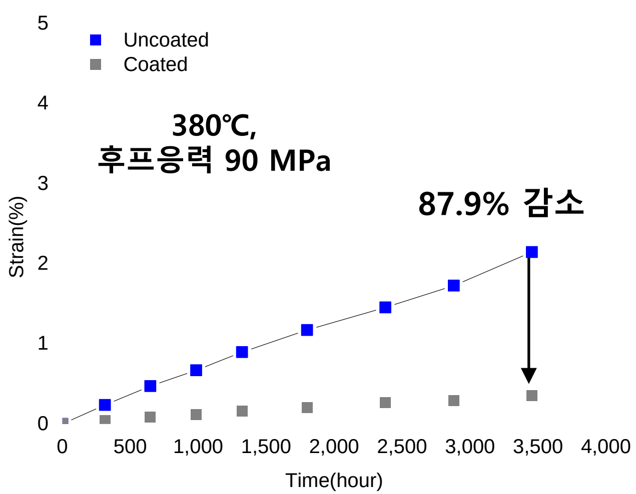

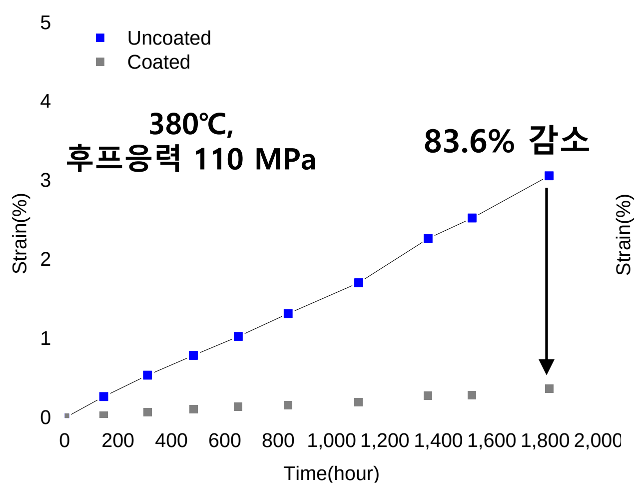

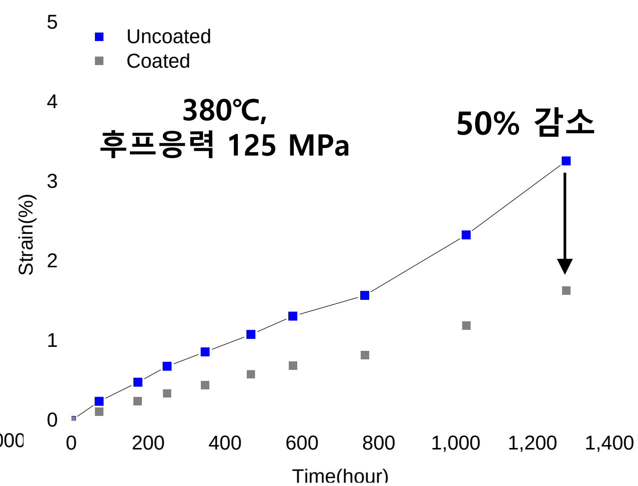

<온도 380℃에서의 피복관 크립 실험 데이터)>

코팅 피복관 고리압축 실험과 코팅 피복관 해석방법론

- 고리압축 실험

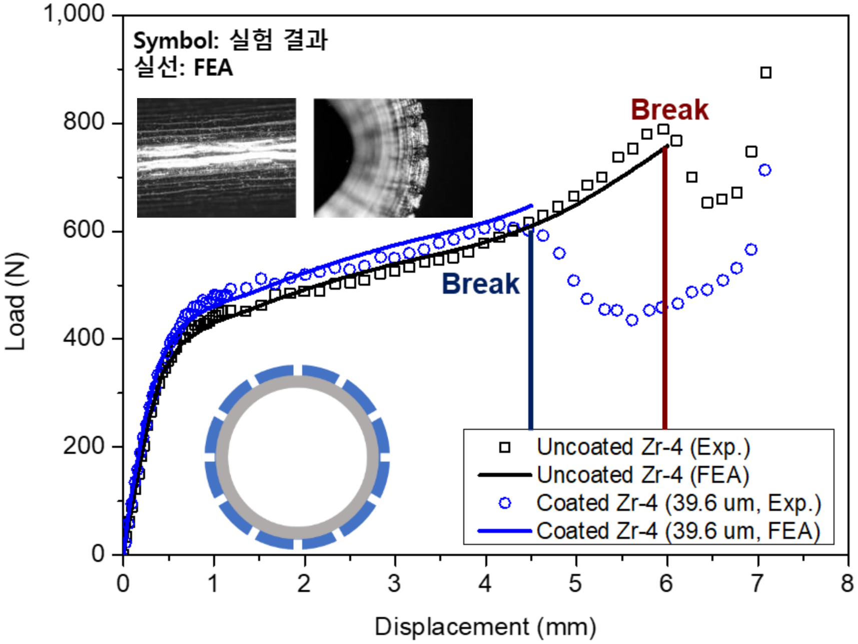

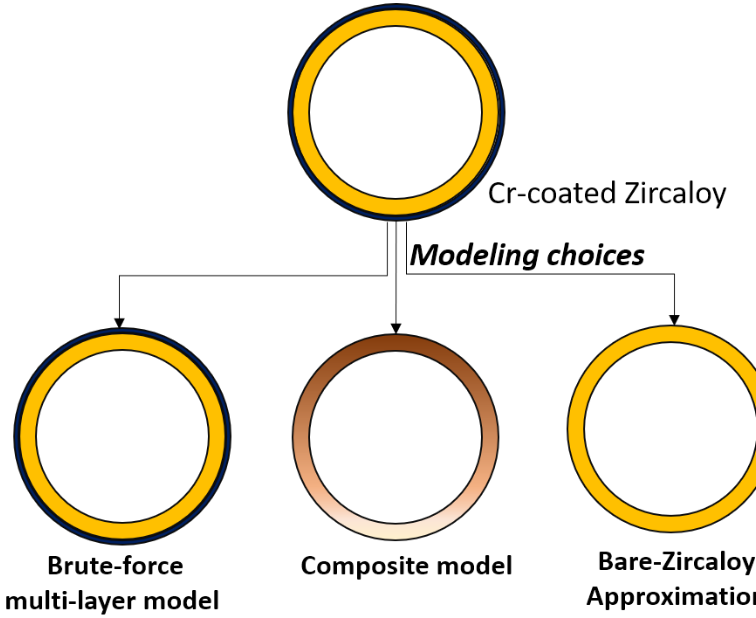

<코팅 피복관 모델링 방법론>

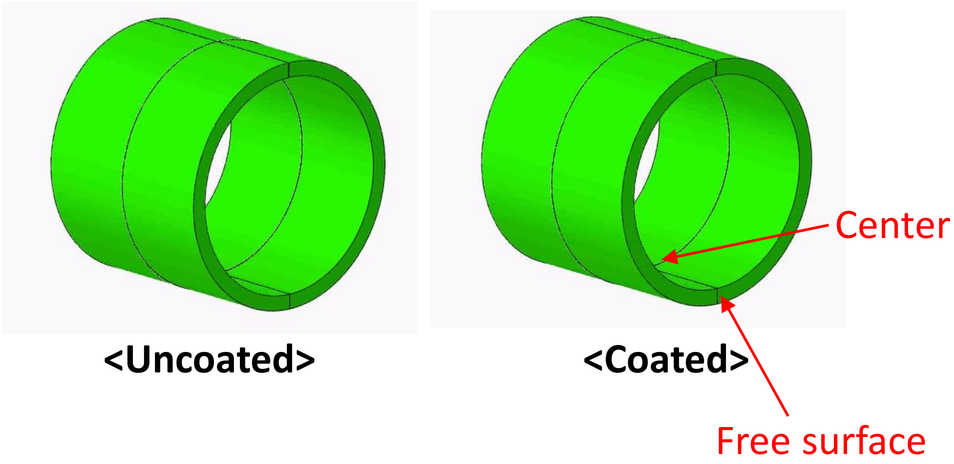

<Uncoated> <Coated>

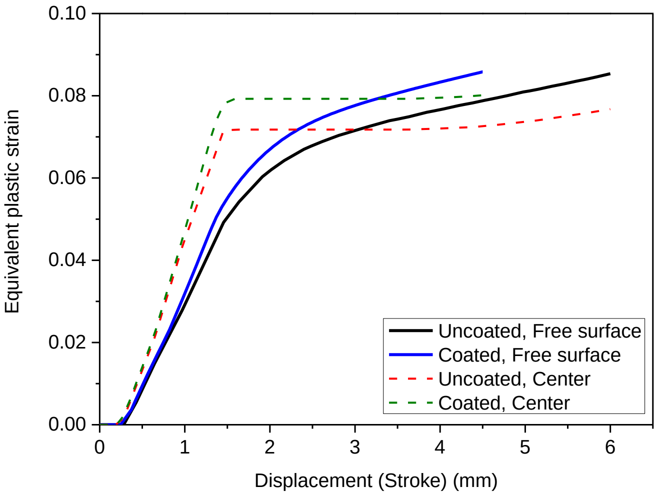

TRANOX : Mechanistic model of Zircaloy oxidation

Current TRANOX 2.0 Capability

- Oxygen distribution, ECR, α and β-phase thickness
- Transient temperature
- Presence of hydrogen (high burnup)
- <u>Pre-transient oxide layer (high burnup)</u>
- Coated cladding

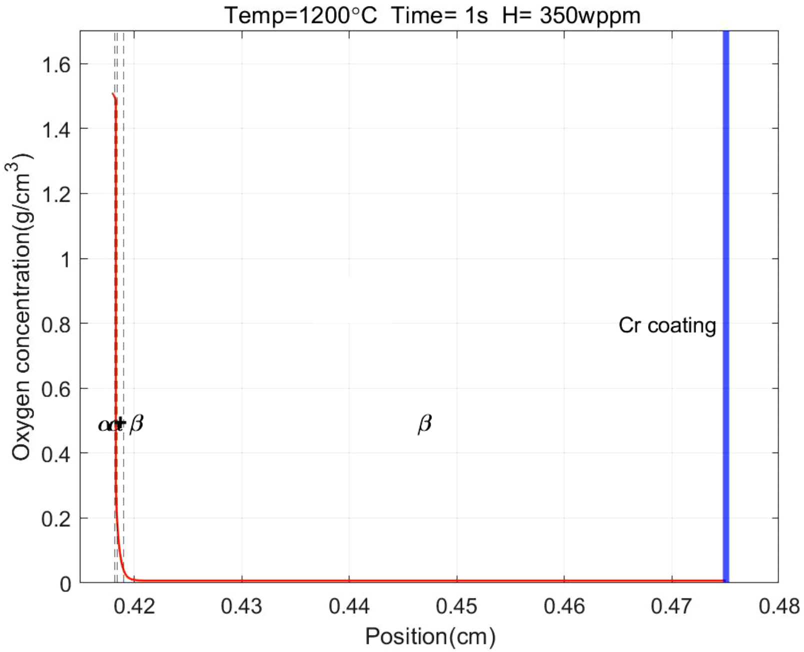

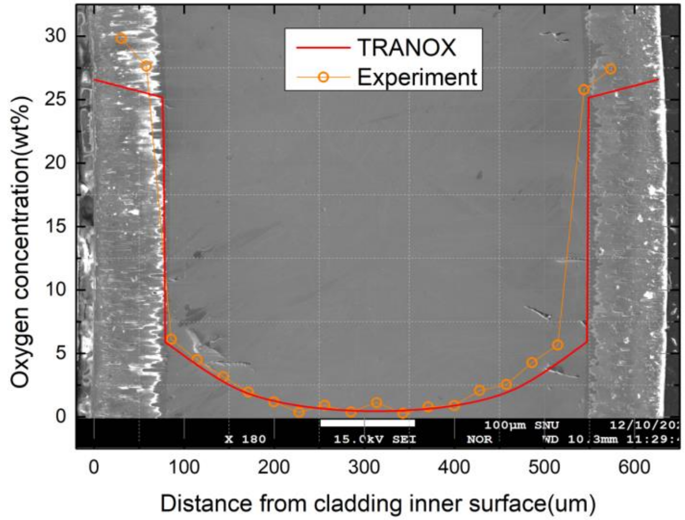

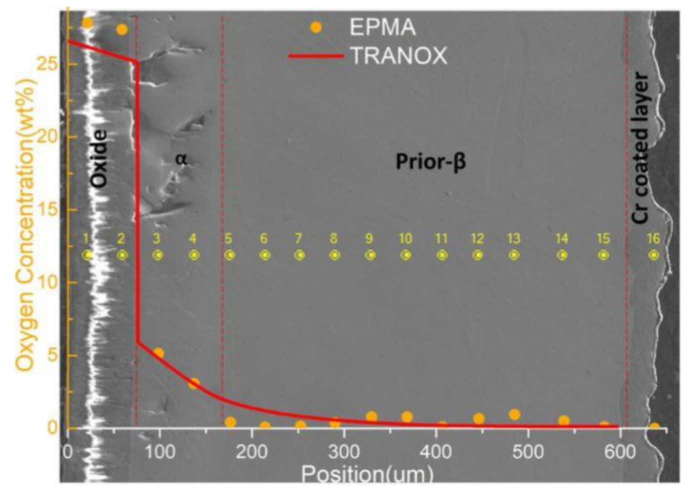

[1] 2021. D. Kim et al., TRANOX: Model for Non-Isothermal Steam Oxidation of Zircaloy Cladding. *Journal of Nuclear Materials* , 556, 153153.
[2] 2022. H. Yook, et al.,. Post-LOCA Ductility of Cr-coated cladding and its embrittlement limit. *Journal of Nuclear Materials*, 558, 153354.
[3] 2022. D. Kim et al., Study of high burnup effect on steam oxidation of Zircaloy and its regulatory implications via the development of pre-transient oxide model of TRANOX. *Journal of Nuclear Materials*, 567,15 153801

Hydrogen migration model

$$\frac{\partial \mathbf{C_{ss}}}{\partial \mathbf{t}} = -\nabla(\mathbf{J_{Fick}} + \mathbf{J_{Soret}}) = -\nabla\left(-\mathbf{D}\nabla\mathbf{C_{ss}} - \frac{\mathbf{Q^{*}DC_{ss}}}{\mathbf{RT^2}}\nabla\mathbf{T}\right)$$

+ mHNGD model for hydride phase change kinetics by Penn State and INL

<mHNGD model of hydrogen phase change kinetics>

Reaction	Condition	Equation
Nucleation	$C_{ss} > TSS_P$	$\frac{\partial C_{ss}}{\partial t} = -K_N(C_{ss} - TSS_P)$ $\frac{\partial C_p}{\partial t} = K_N(C_{ss} - TSS_P)$
Growth	$C_{ss} > TSS_D$ & $C_p > 0$	$\frac{\partial x}{\partial t} = -K_G p(1-x)(-\ln(1-x))^{1-\frac{1}{p}}$ $\frac{\partial C_{ss}}{\partial t} = -\frac{\partial C_p}{dt}, x = \frac{C_p}{C_{tot} - TSS_D}$
Dissolution	$C_{ss} < TSS_D$ & $C_p > 0$	$\frac{\partial C_{ss}}{\partial t} = K_D(C_{ss} - TSS_D)$ $\frac{\partial C_p}{dt} = -K_p(C_{ss} - TSS_D)$
Phase equilibrium	Else	$\frac{\partial C_{SS}}{\partial t} = \frac{\partial C_p}{\partial t} = 0$

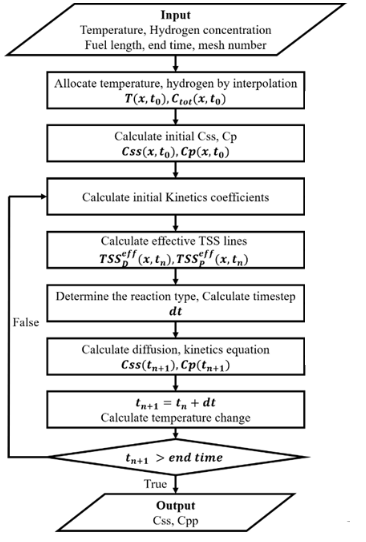

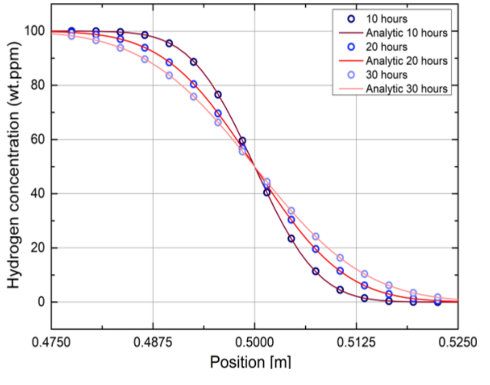

<Code verification>

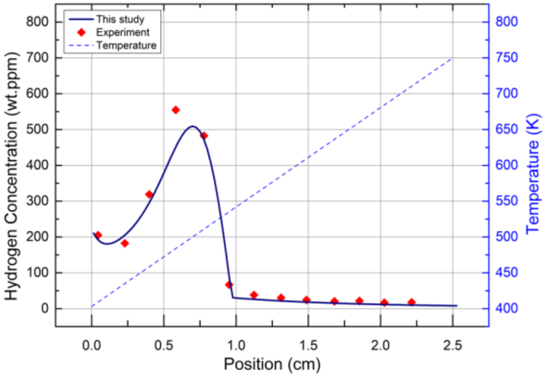

<Validation Sawatzky's experiment>

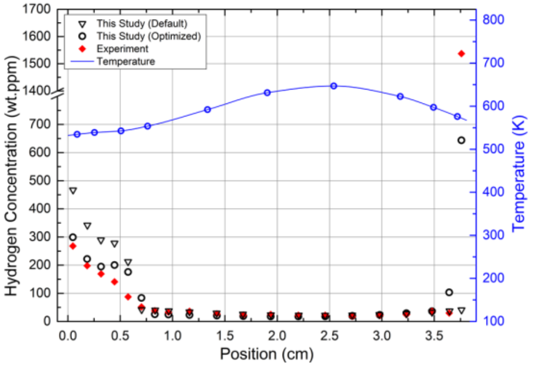

<Validation Kammenzind experiment>

Spent fuel simulation module of GIFT

- **Spent fuel simulation module**
  - Dry storage pellet swelling
  - Dry storage cladding creep
    (EDF Creep correlation)
  - Dry storage temperature distribution
  - Hydrogen transport model (mHNGD model newly incorporated)

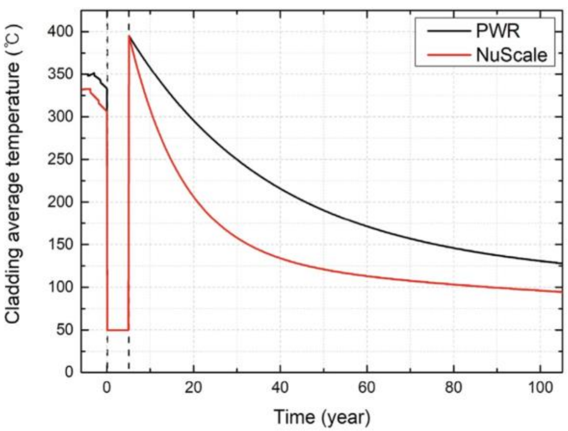

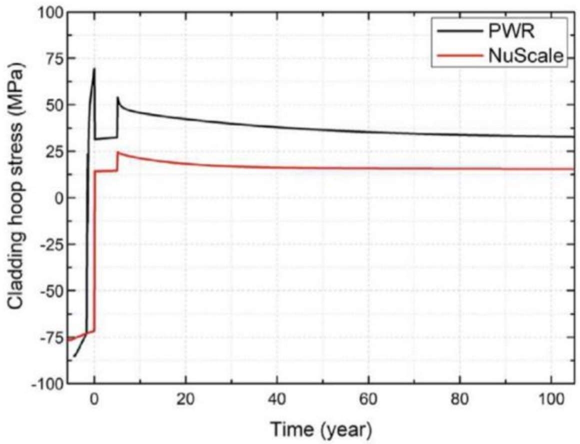

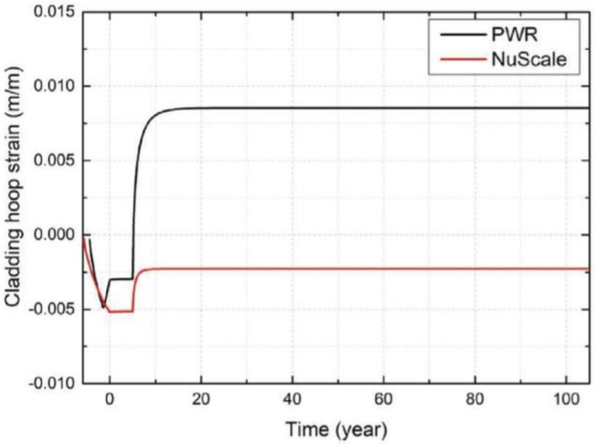

- **Simulation of spent fuel in a continuous manner from the steady-state operation**

2022. D. Woo and Youho Lee., Spent fuel simulation during dry storage via enhancement of FRAPCON-4.0: Comparison between PWR and SMR and discharge burnup effect. Nuclear Engineering and Technology

Other pellet and cladding model features

- **Gd_2O_3 central pellet for i-SMR fuel**
  - Simulation for soluble boron free SMR(e.g., i-SMR, Korea)
  - Elementary model that captures the thermal effect of the central void
  - Further improvement is possible upon the availability of UO_2-Gd_2O_3 reaction and resulting effects.

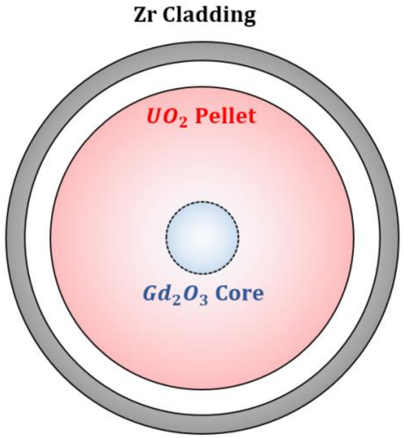

- **Multi-layered SiC composite cladding**
  - State-of-the arts SiC cladding models/properties a
  - Pseudo-ductile behavior of SiC composite
  - Statistical failure probability

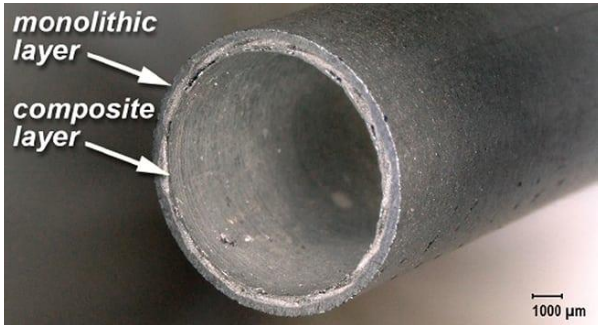

[1] 2022. Hyuntaek Rho, Youho Lee. Development of a 2D Axisymmetric SiC Cladding Mechanical Model and its Applications for Steady-State and LBLOCA Analysis. Journal of Nuclear Materials, 558, 153311.

Code interface: input, and output

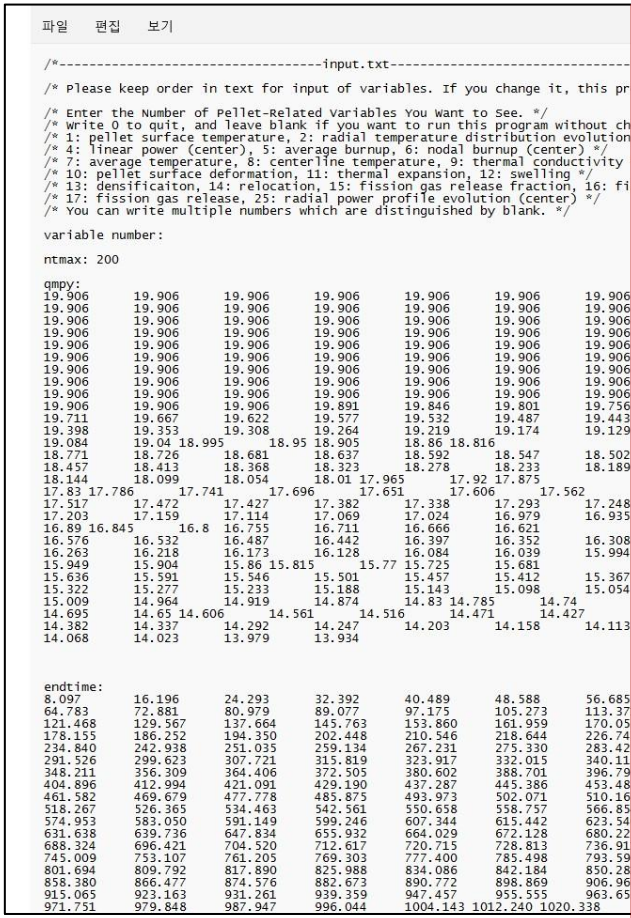

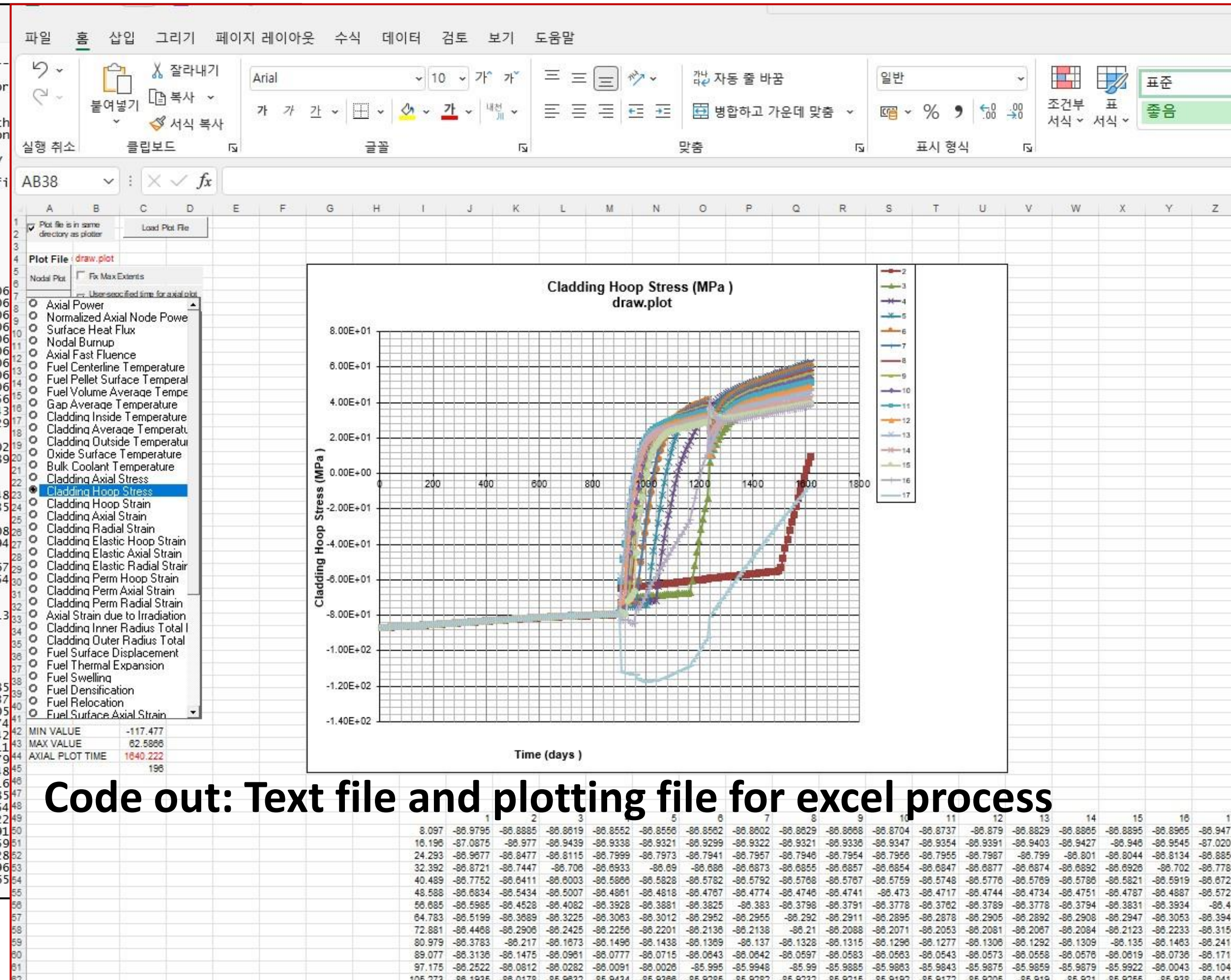

Code out: Text file and plotting file for excel process

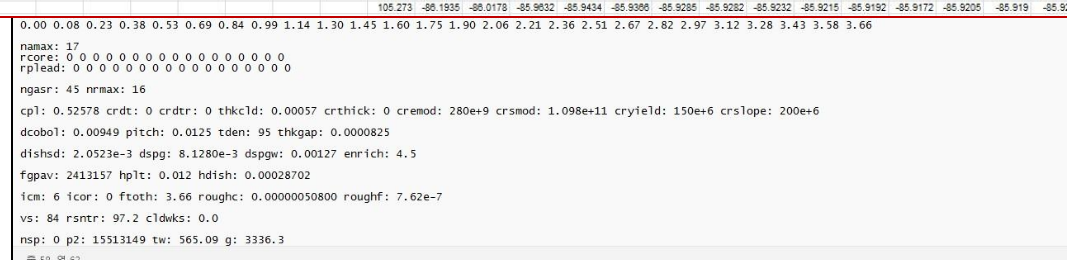

Code input: Text file

Introduction of GIFT code

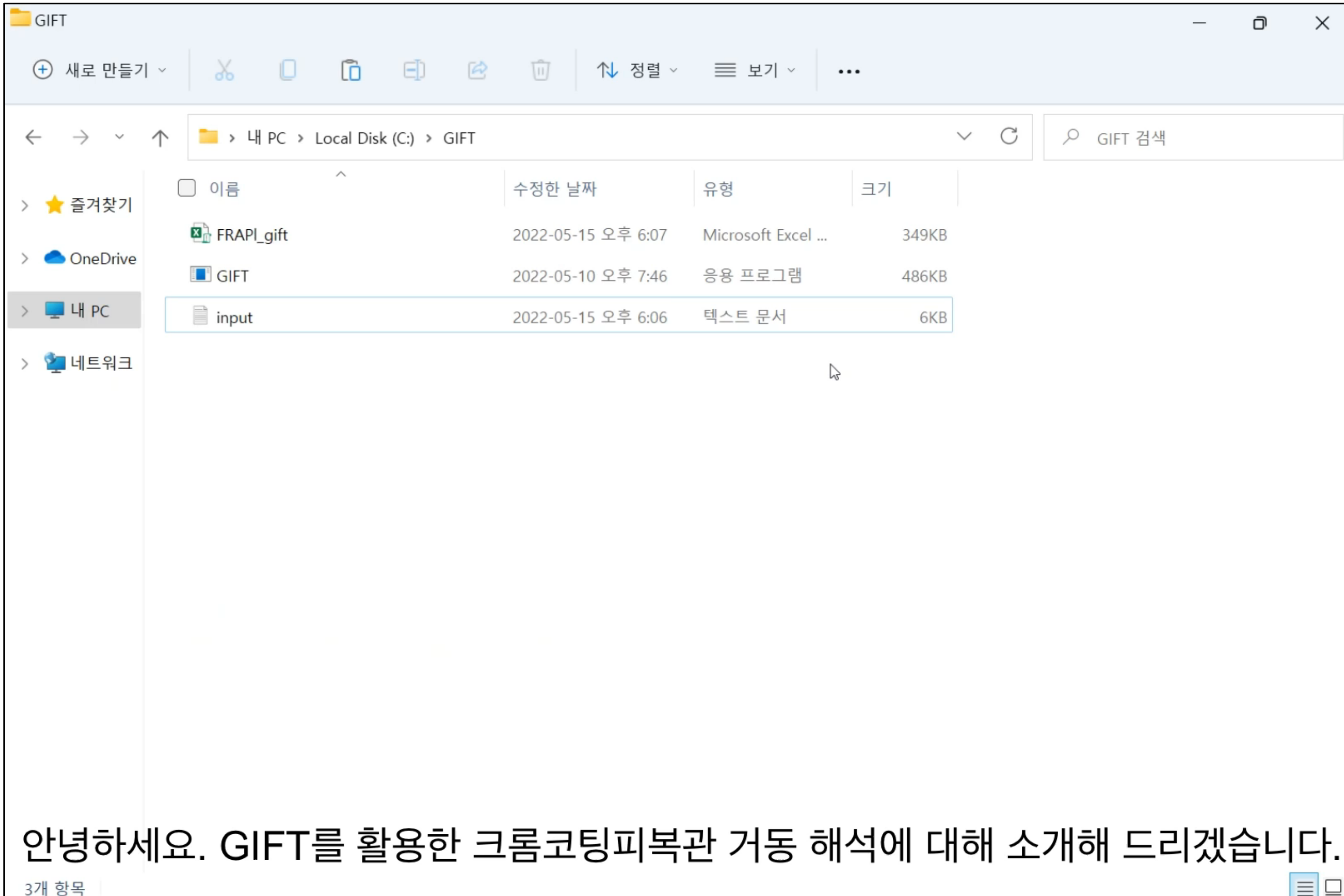

Bare Zr vs. Cr-Coated Zr (16um)

Average power

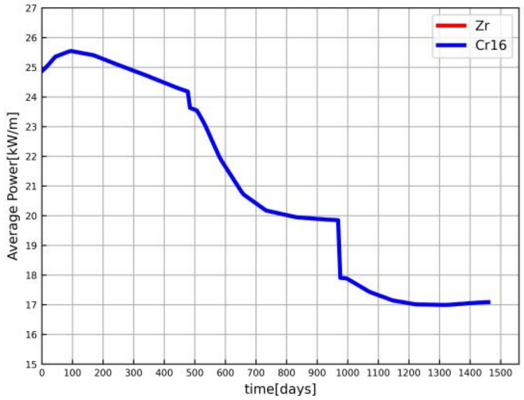

Rod average burnup

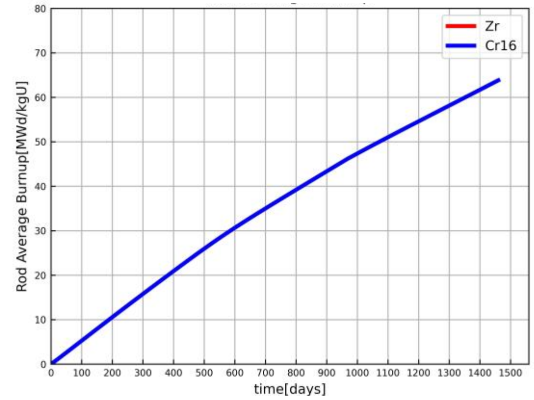

Fission gas release

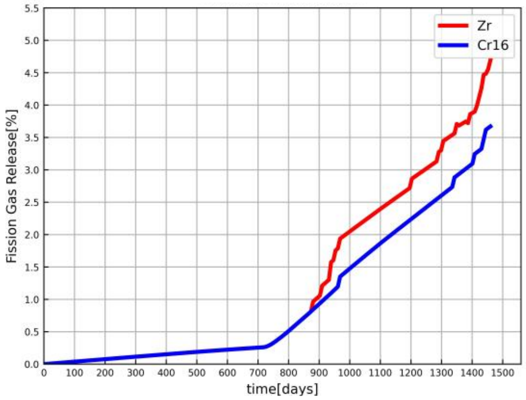

Cladding hoop stress

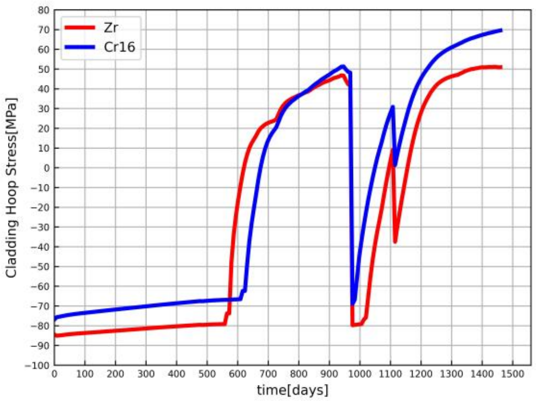

Cladding hoop strain

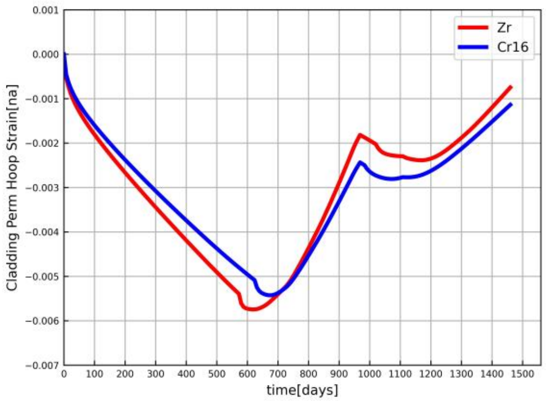

Mechanical gap

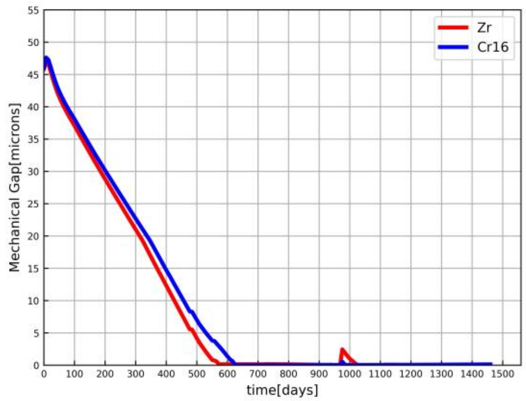

PWR vs. NuScale

Average power

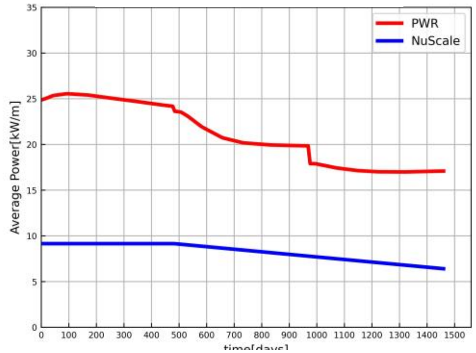

Rod average burnup

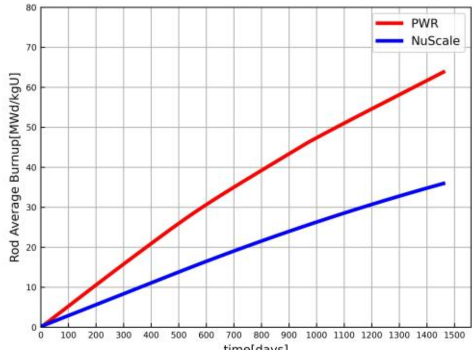

Fission gas release

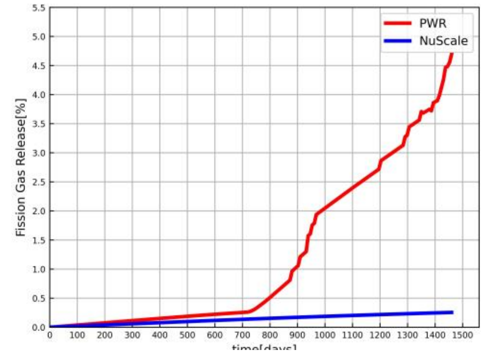

Cladding hoop stress

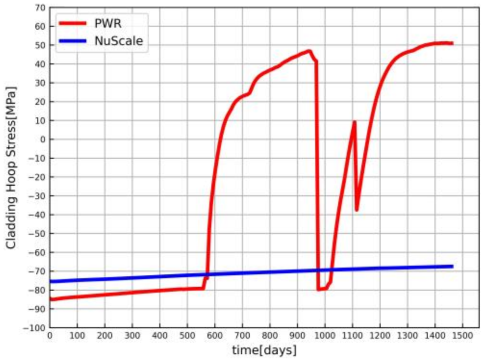

Cladding hoop strain

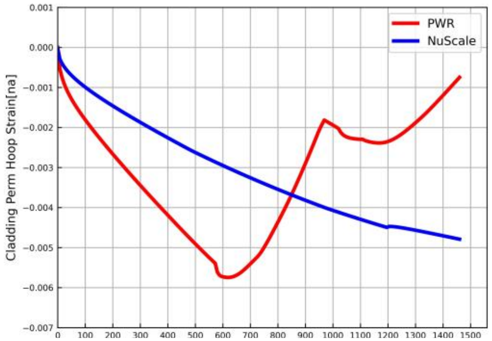

Mechanical gap

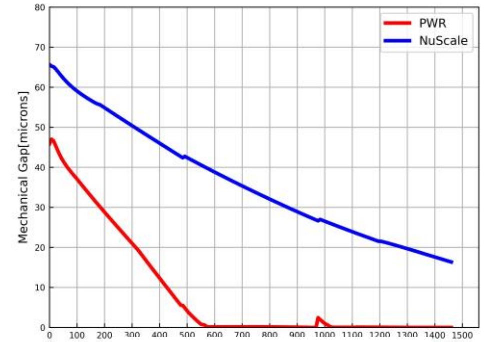

Hydrogen concentration

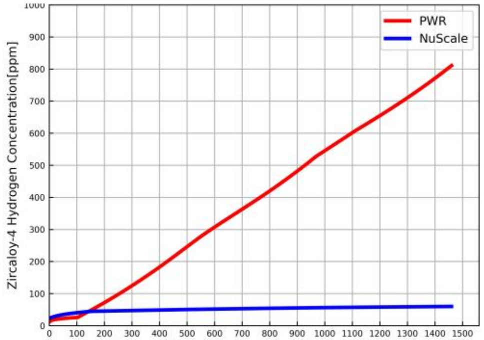

Oxide thickness

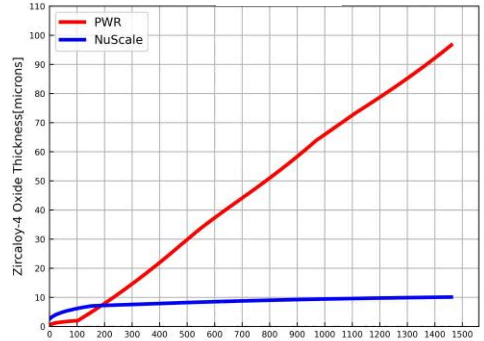

Zr-4 vs. SiC (CMC)

Average power

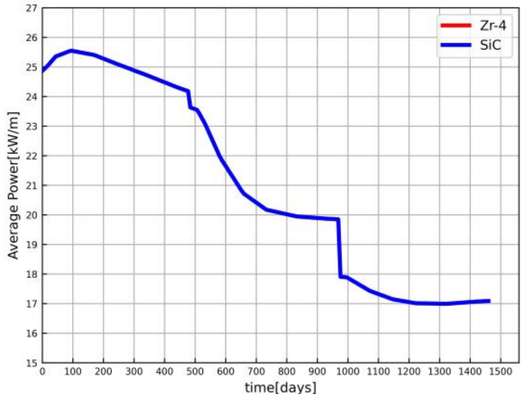

Rod average burnup

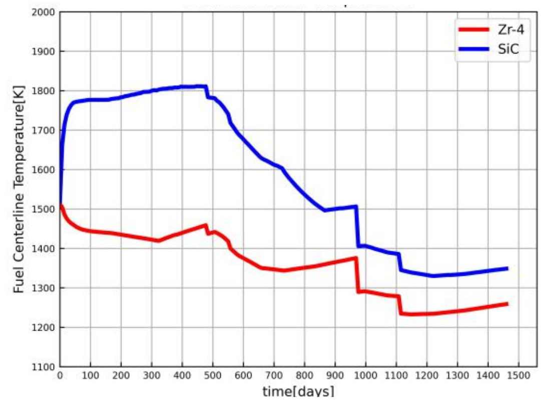

Fission gas release

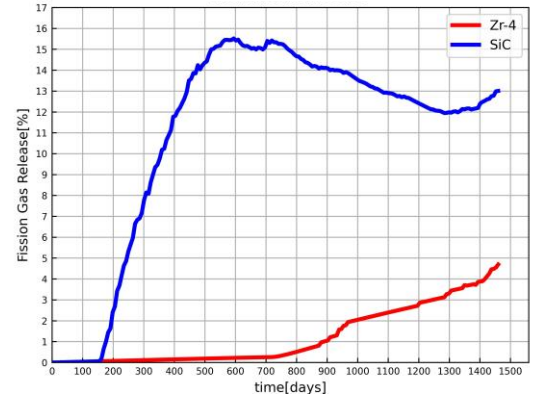

Cladding hoop stress

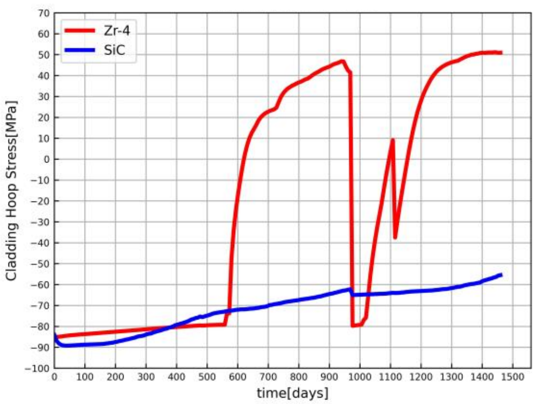

Cladding hoop strain

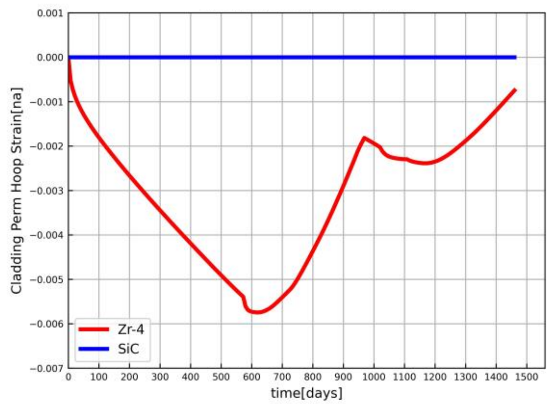

Mechanical gap

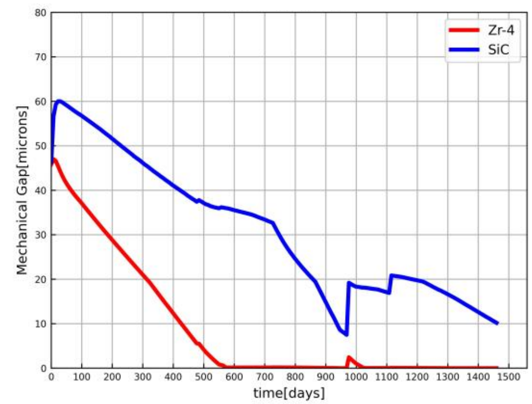

2. Image analysis of hydrided Zircaloy

High burnup nuclear fuel characteristics

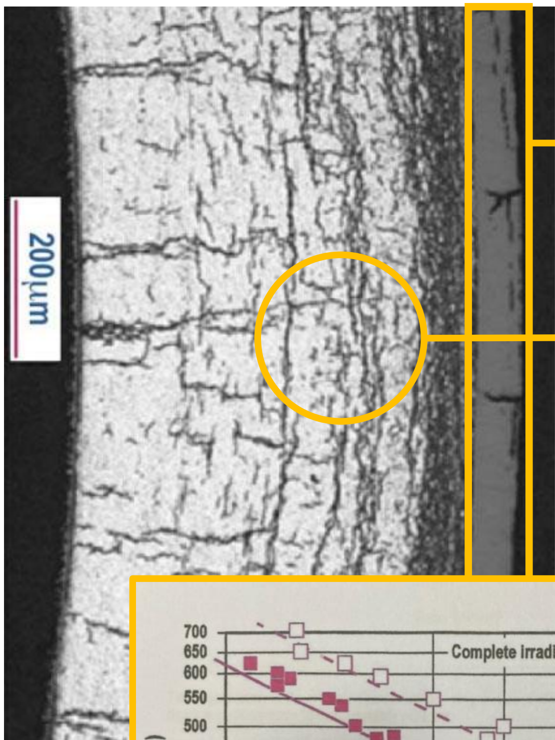

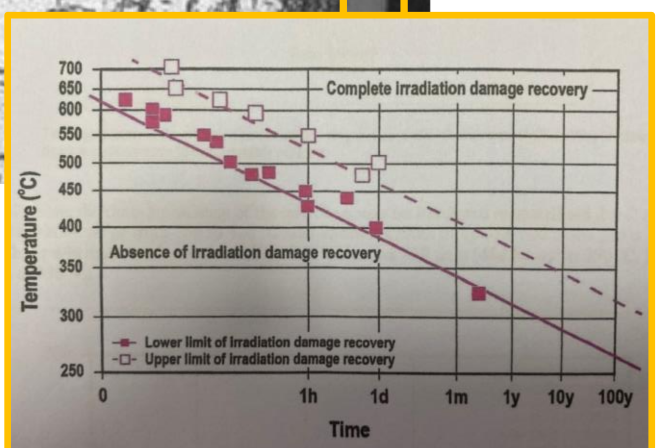

① Thick oxide layer (limited to ~100μm)

- Steady-state corrosion
- No load carrying capability, hence effectively ~16% thickness reduction effect in load carrying capability
- No-oxygen diffusion into Zr matrix in steady-state (~350℃)
- Oxygen may diffuse into Zr matrix in accident (>1000℃)

Degrading load carrying capability in a limited extent based on the oxide scale thickness

② Hydride formation

- Hydrogen pick up as a consequence of steady-state corrosion and following precipitation
- Formation of FCC phase
- Degrades the mechanical strength Zr matrix

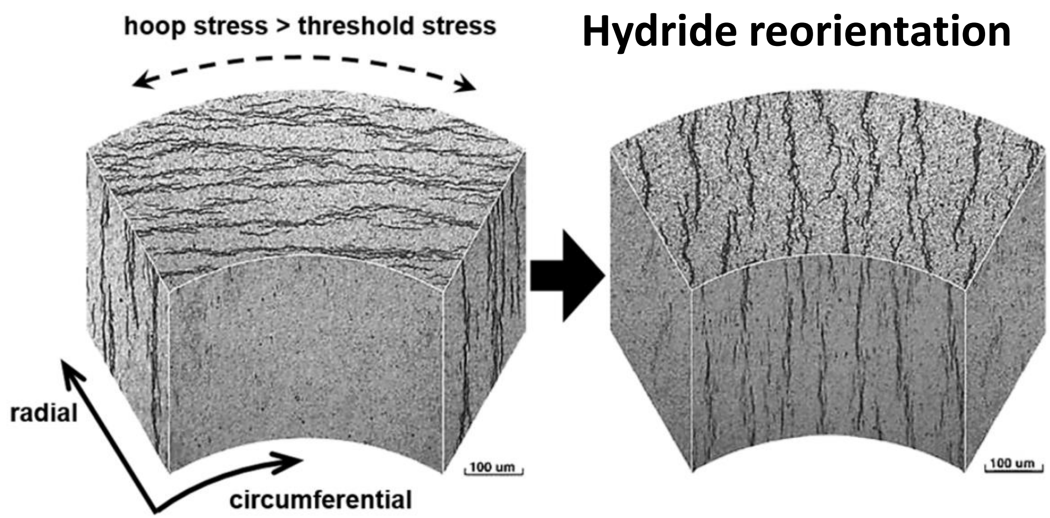

PROPHET : SNU-developed hydride image analysis code

(a)

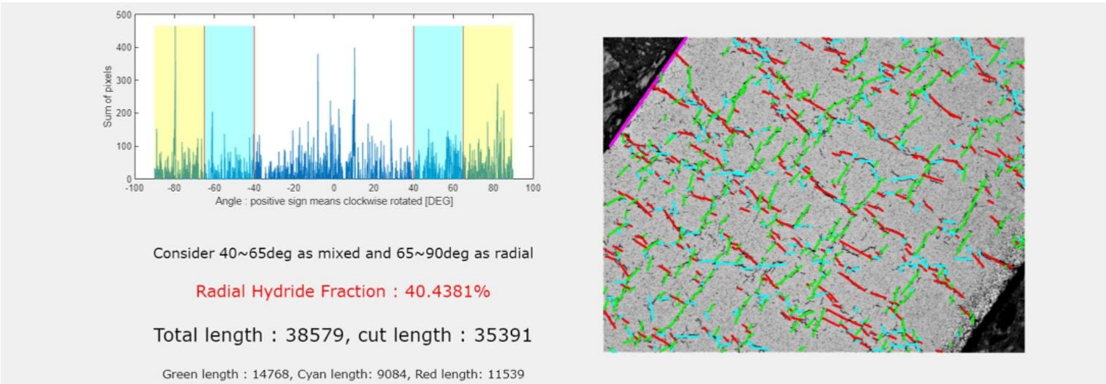

Radial Hydride Fraction (RHF)

$$RHF = \frac{\sum_i L_i f_i}{\sum_i L_i}$$

$$f_i = \begin{cases} 0:\ 0° \le \theta < 40°:\ circumferential \\ 0.5:\ 40° \le \theta < 65°:\ mixed \\ 1:\ 65° \le \theta < 90°:\ radial \end{cases}$$

(b)

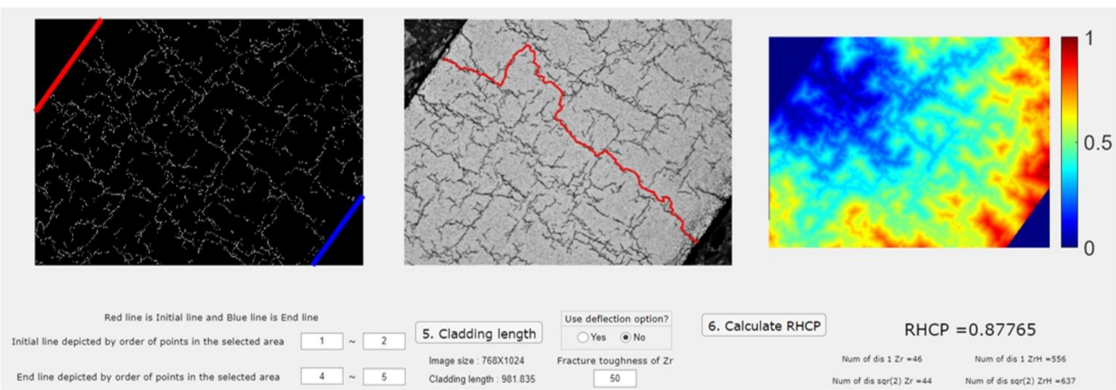

Radial Hydride Continuous Path (RHCP)

$$RHCP = \frac{Lw_{Zr} - (x_{Zr}w_{Zr} + x_{ZrH}w_{ZrH})}{L(w_{Zr} - w_{ZrH})}$$

Relative cost of Zr matrix and hydride:

$w_{Zr} = 50\ MPa\sqrt{m}, \qquad w_{ZrH} = 1\ MPa\sqrt{m}$

0= Minimum cost path consists of 100% Zr matrix (Straight Zr path)

1= Minimum cost path consists of 100% ZrH (Straight hydride path)

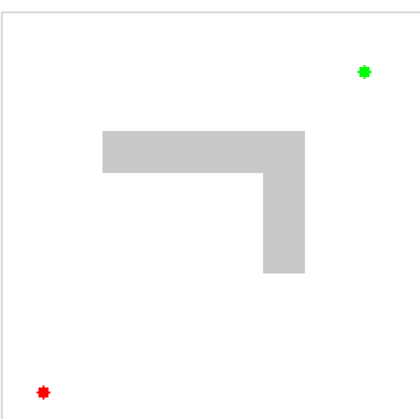

Dijkstra's algorithm:
Finding the least-cost path

[D. Kim, D. Kim, D. Woo, Y. Lee, Journal of Nuclear Materials 564 (2022) 153647]

PROPHET : SNU-developed hydride image analysis code

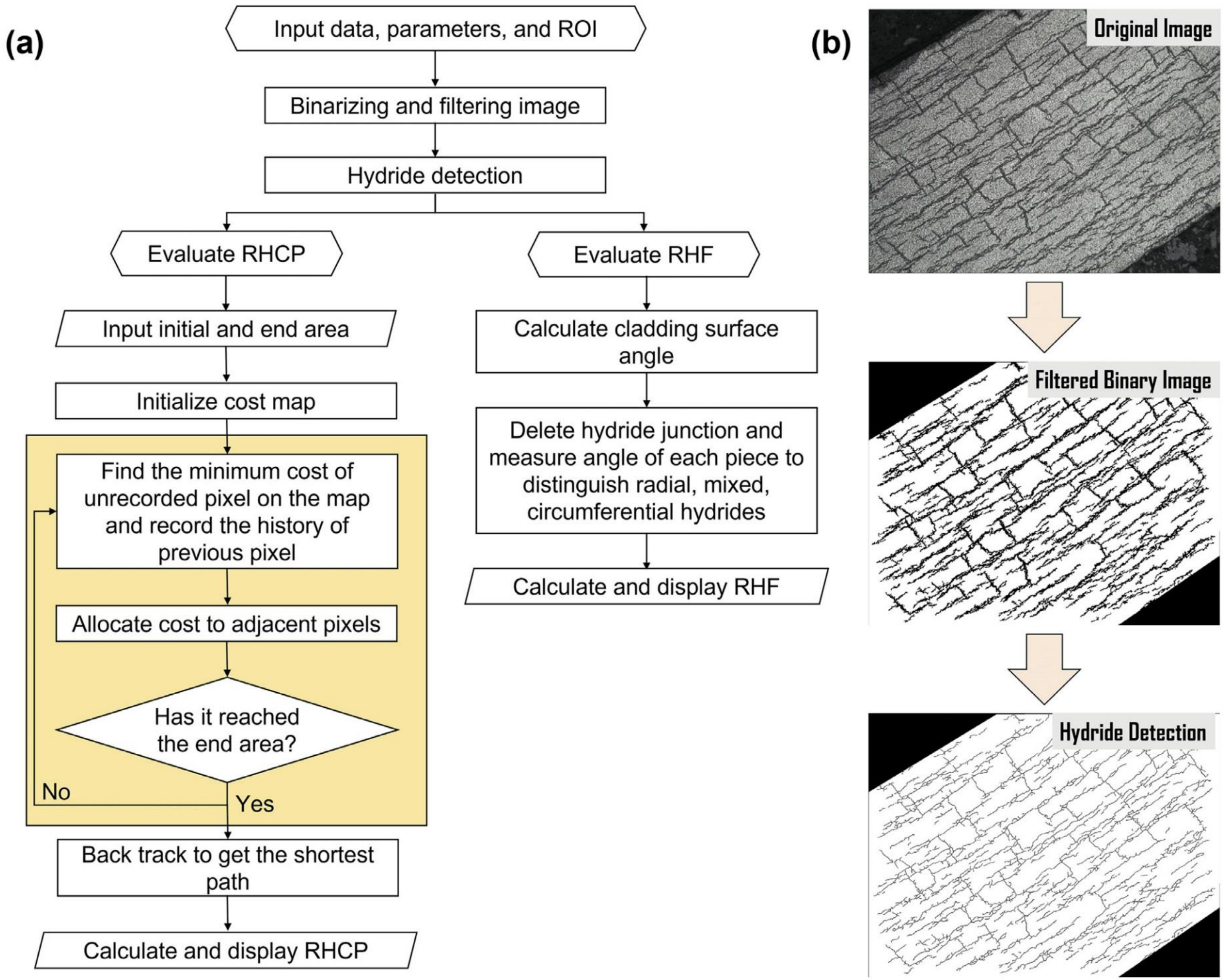

PROPHET : SNU-developed hydride image analysis code

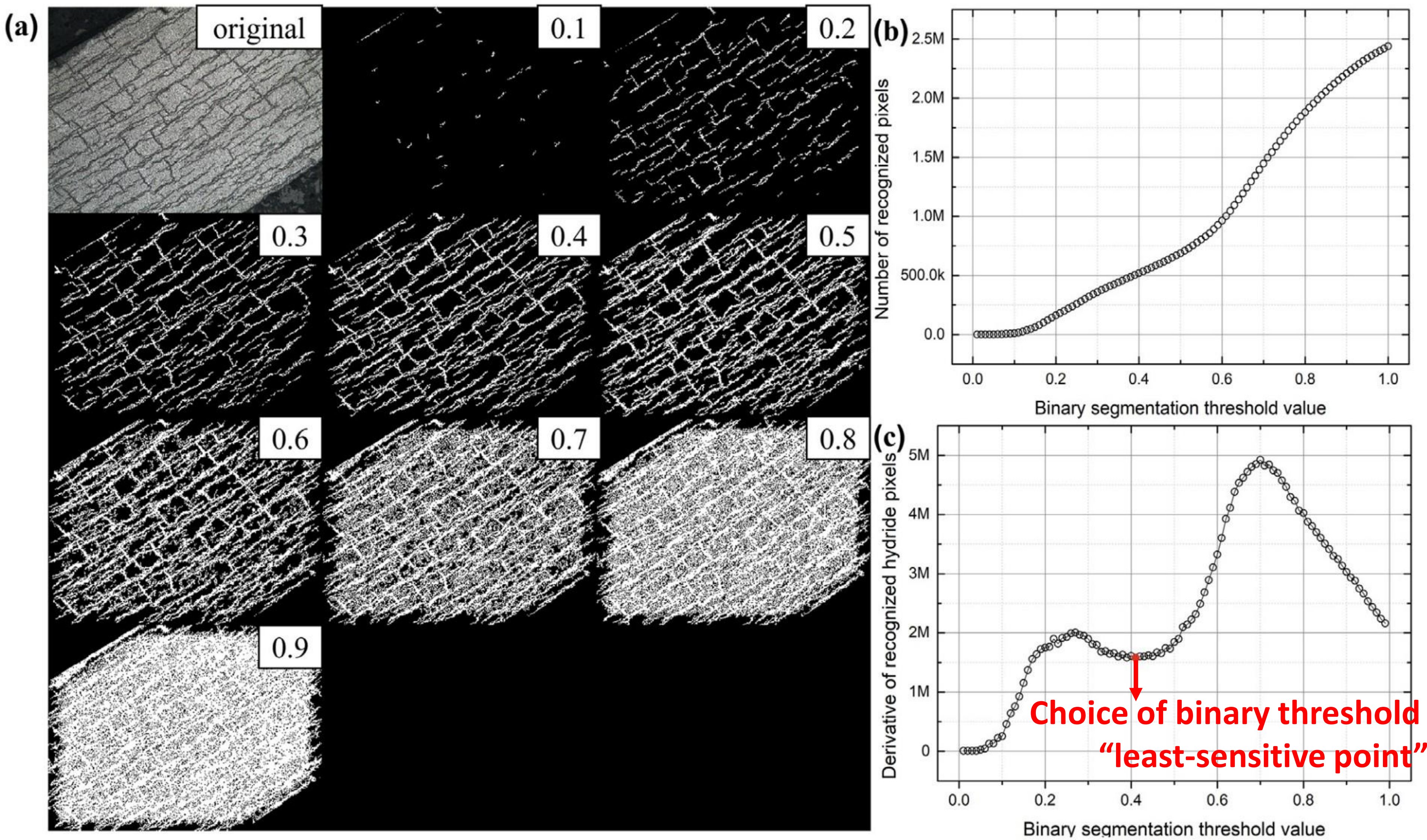

PROPHET : SNU-developed hydride image analysis code

- **RHCP assessment of various hydride morphologies**

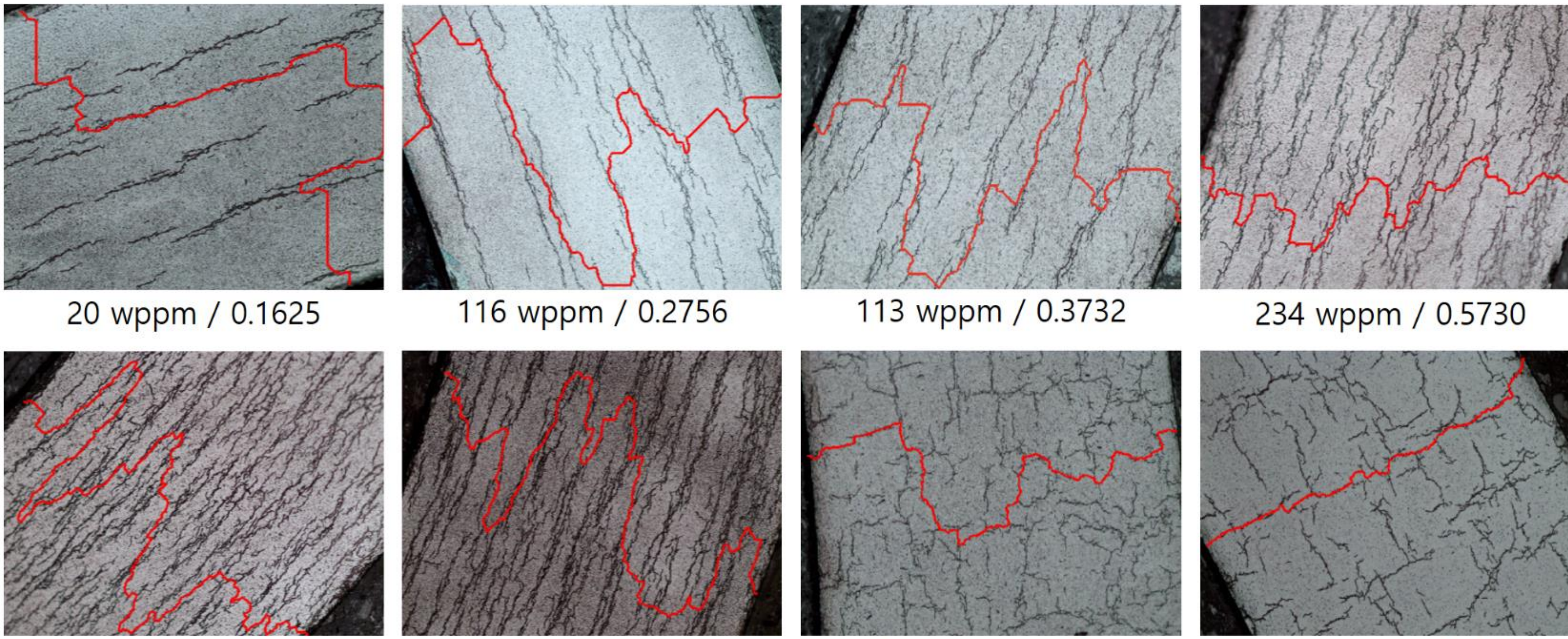

668 wppm / 0.6726

307 wppm / 0.7705

186 wppm / 0.8519

83 wppm / 0.94

PROPHET : SNU-developed hydride image analysis code

- **RHF assessment of various hydride morphologies using PROPHET**

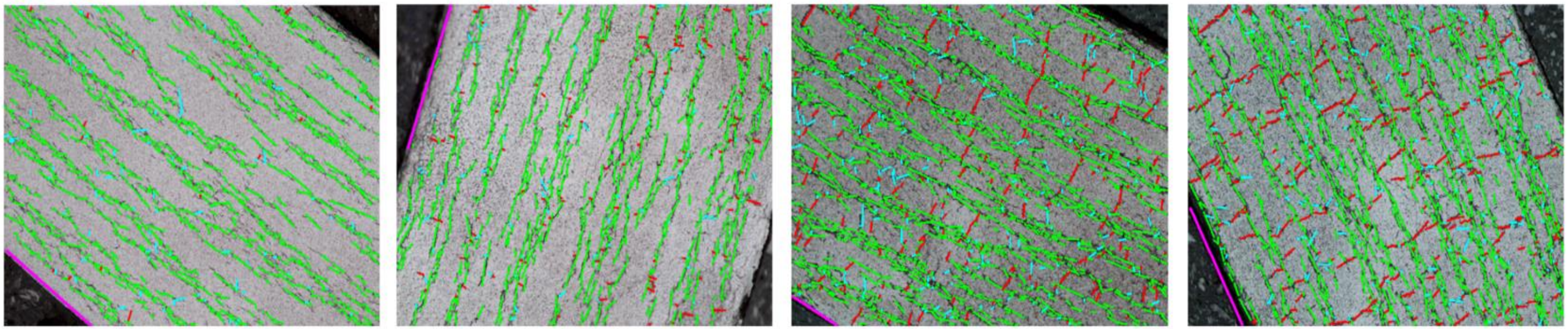

229 wppm / 0% | 233 wppm / 4.9% | 381 wppm / 11.9% | 466 wppm / 15.9%

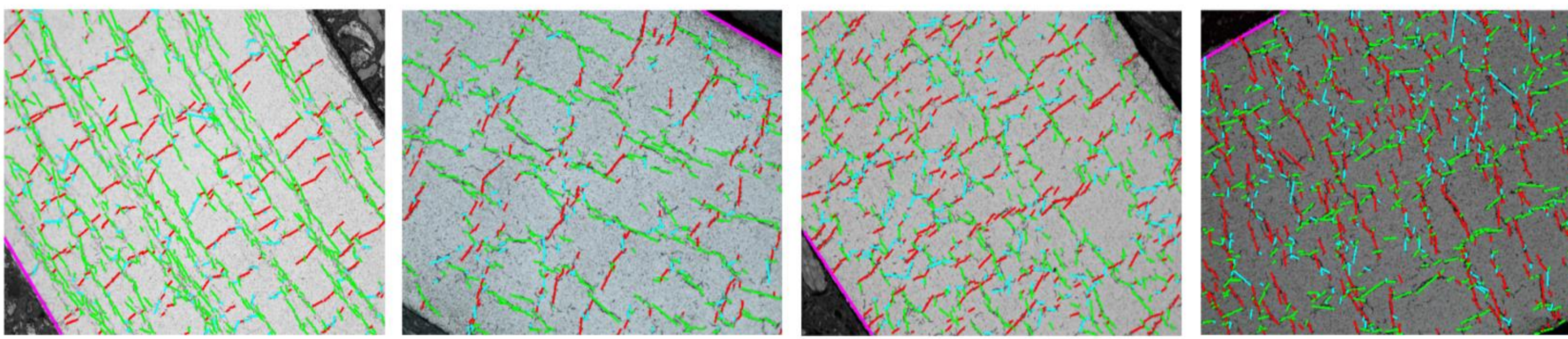

312 wppm / 21.0% | 187 wppm / 27.6% | 171 wppm / 39.1% | 167 wppm / 46.5%

PROPHET is accessible at our website

- **PROPHET is open to public via http://fuel.snu.ac.kr.**

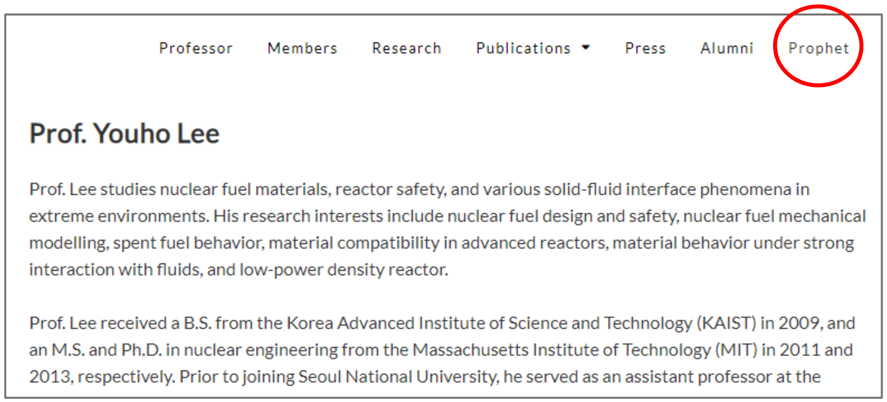

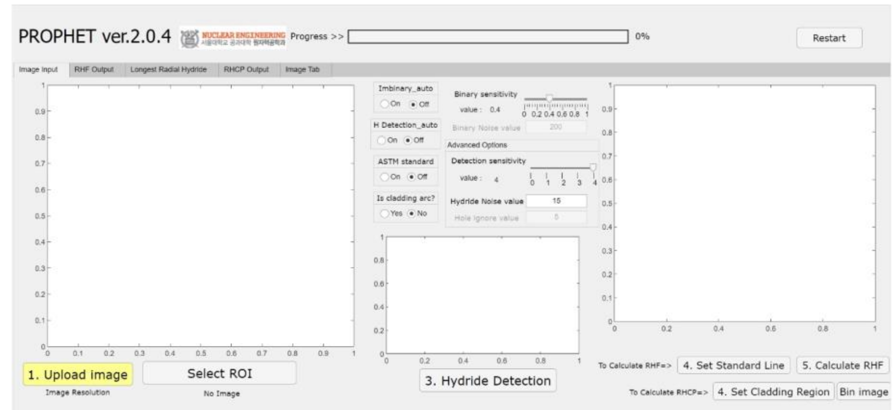

<working screen of PROPHET>

- **Statistical nature of image analysis:**

For both RHF and RHCP, the results in four directions were averaged and used.

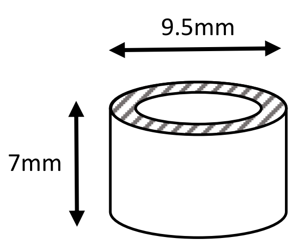

<Cladding tube>

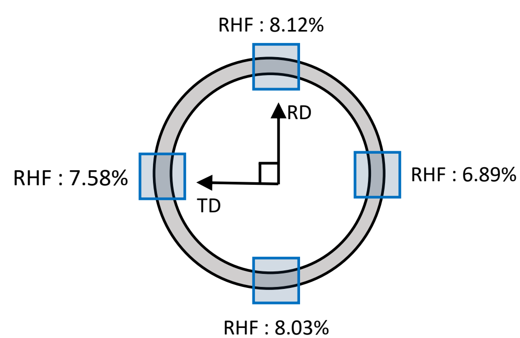

<Average RHF : 7.65%>

Hydride reorientation

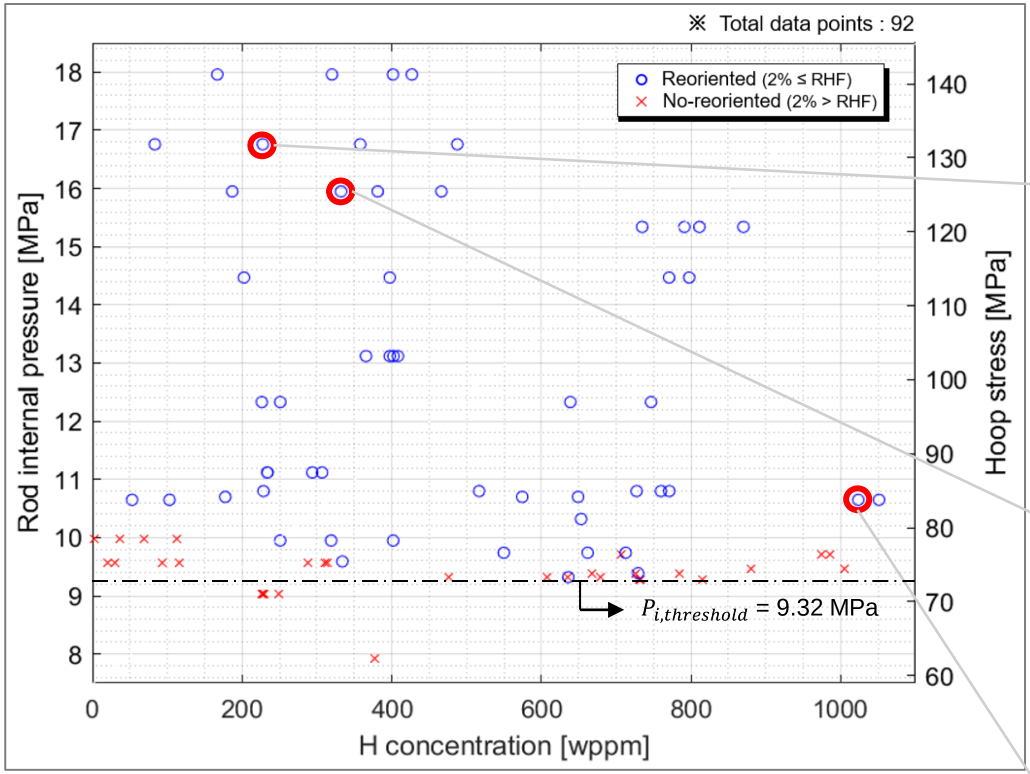

<Hydride reorientation with regard to hydrogen contents and rod internal pressure>

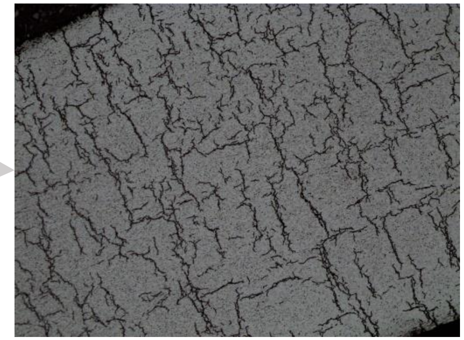

17.96 MPa, 206.9 wppm, 46.01%

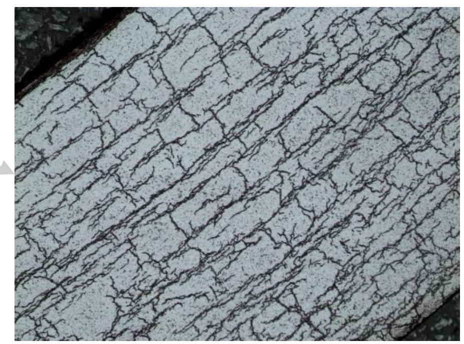

16.76 MPa, 357.9 wppm, 14.05%

10.8 MPa, 1023.6 wppm, 3.13%

- Hydride reorientation occurs with P_i > 9.32 MPa (>73.3 MPa of hoop stress).

- The slightly early reorientation is considered due to the multi-stress state and constant pressure.

Structural integrity with various hydride morphologies

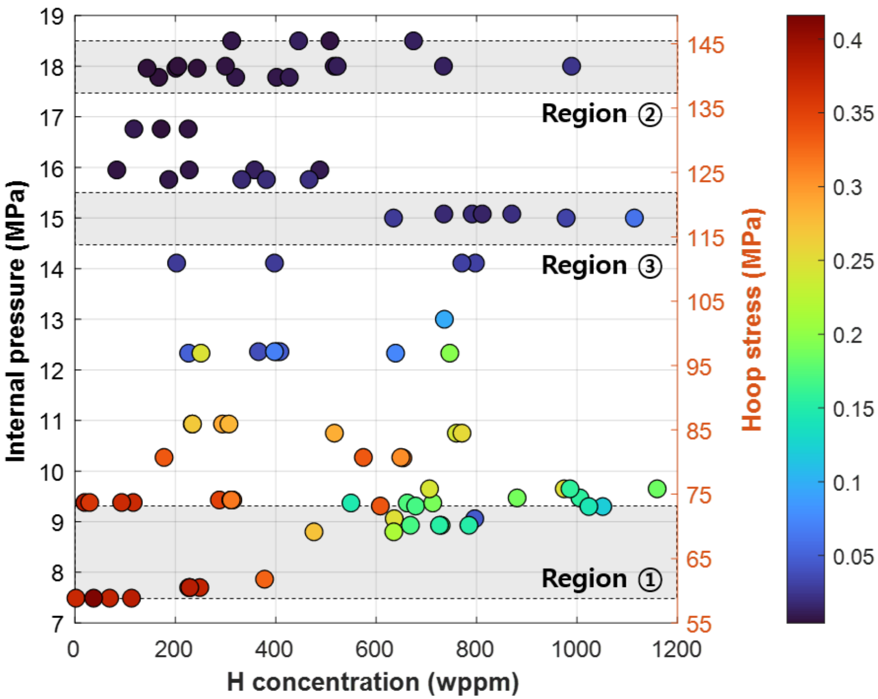

<Strain Energy Density (SED) of various hydride morphologies induced by various H concentration and applied pressure >

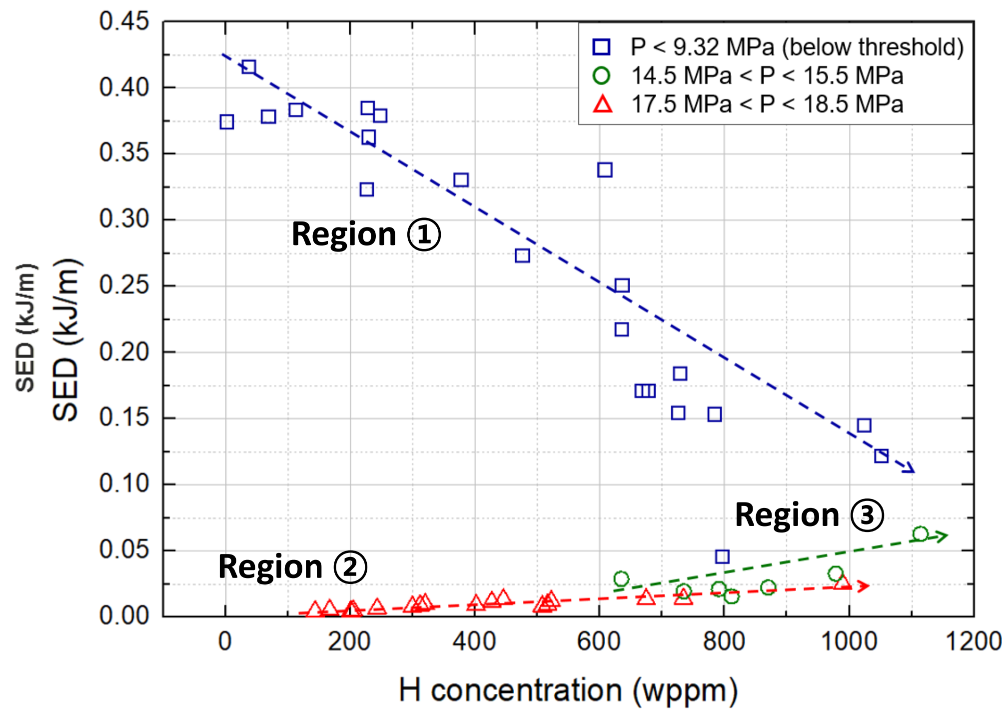

<SED change with H concentration along Region ① (below reorientation threshold) and Region ② (well above reorientation threshold)>

- Hydrogen concentration is a key parameter for Zircaloy without hydride reorientation.
- With a presence of appreciable radial hydrides, the strength exhibits a complex behavior: Increasing H concentration is shown to increase SED (i.e., Region ②)

Beneficial effect of circumferential hydrides

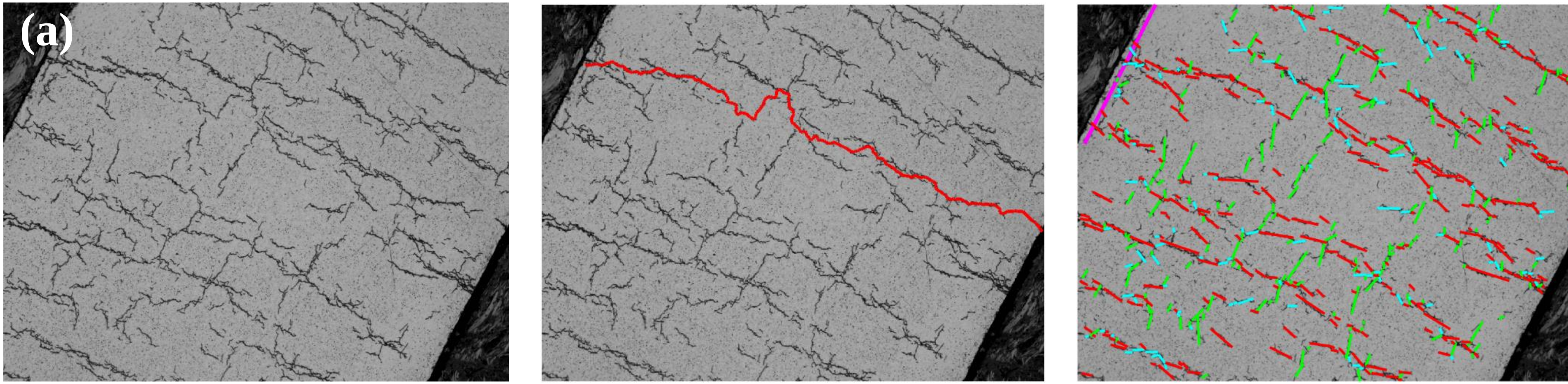

143.7 wppm / 18 MPa RHCP = 0.902 **SED=4 J/m** RHF = 47.3%

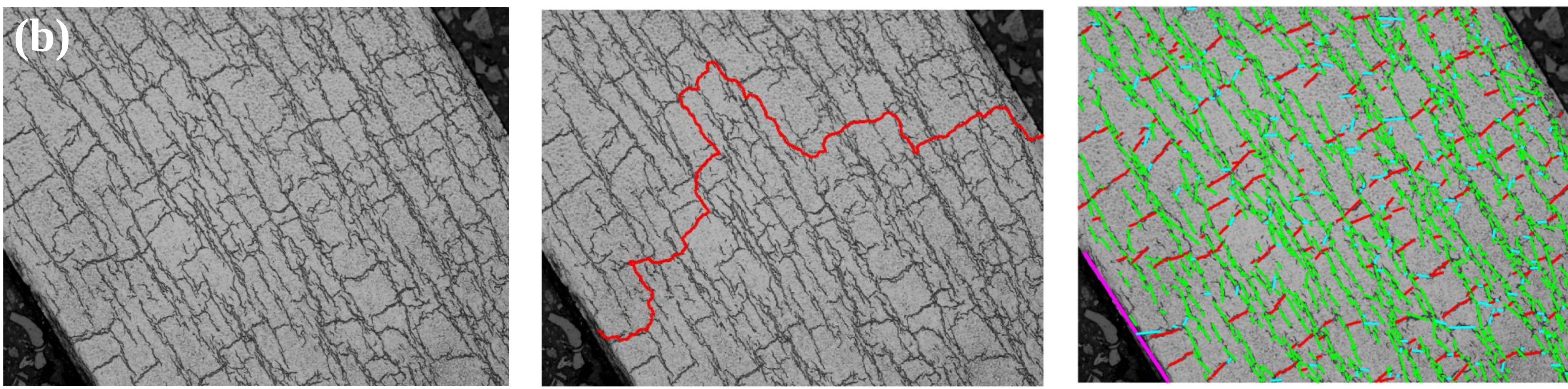

522.4 wppm / 18 MPa / 0.012 kJ/m RHCP = 0.883 **SED=12J/m** RHF = 15.9%

<OM, RHF, RHCP images for applied pressure of 18 MPa: (a) low total hydrogen case of 143.7 wppm, (b) high total hydrogen case of 522.4 wppm>

Mechanisms of circumferential hydride-aided strength

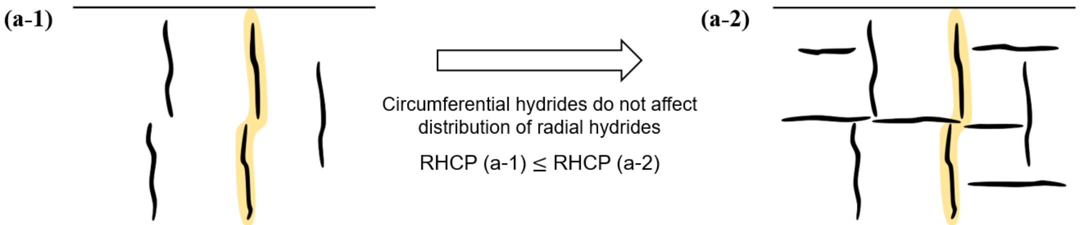

<Ideal case: introduction of circumferential hydrides without affecting radial hydrides>

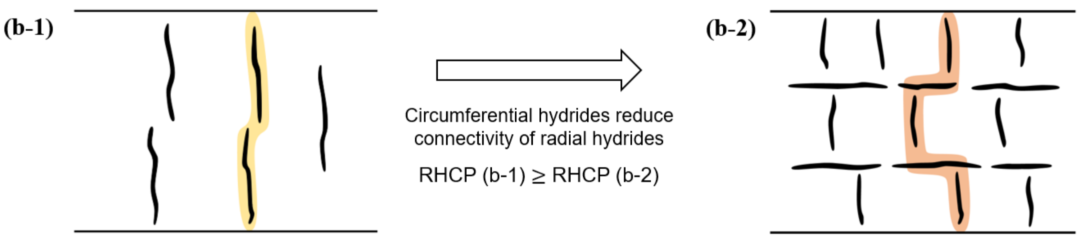

<Real case: introduction of circumferential hydrides decrease radial hydride connectivity>

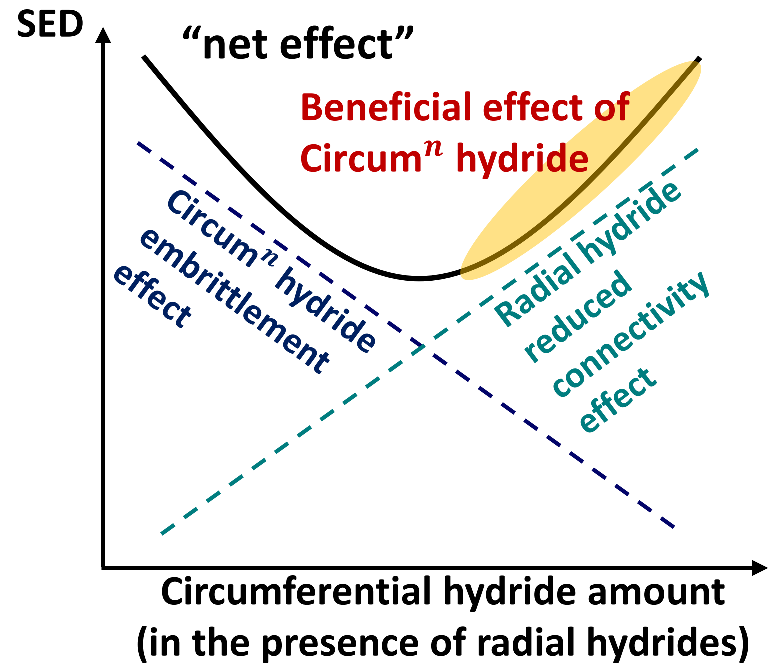

<Schematic diagram of two competing mechanisms of circumferential hydrides on SED in the presence of radial hydrides >

Effect of increasing circumferential hydrides in the presence of radial hydrides:

①: Increasing embrittlement (strength ↓)

②: Decreasing radial hydride connectivity (strength ↑)

RHF (>5%) is a powerful metric

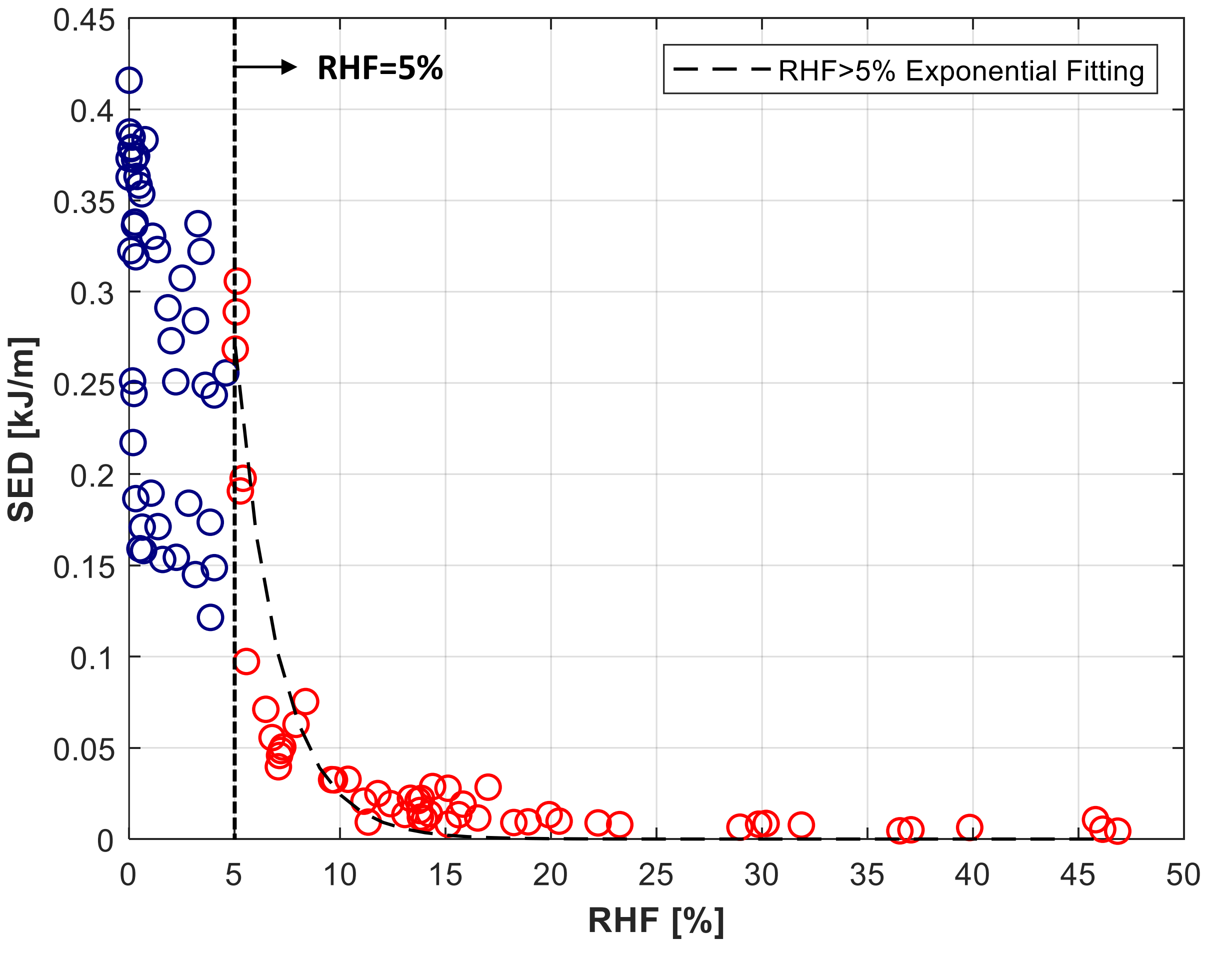

<SED change with RHF>

Predictability of SED with H concentration and RHCP

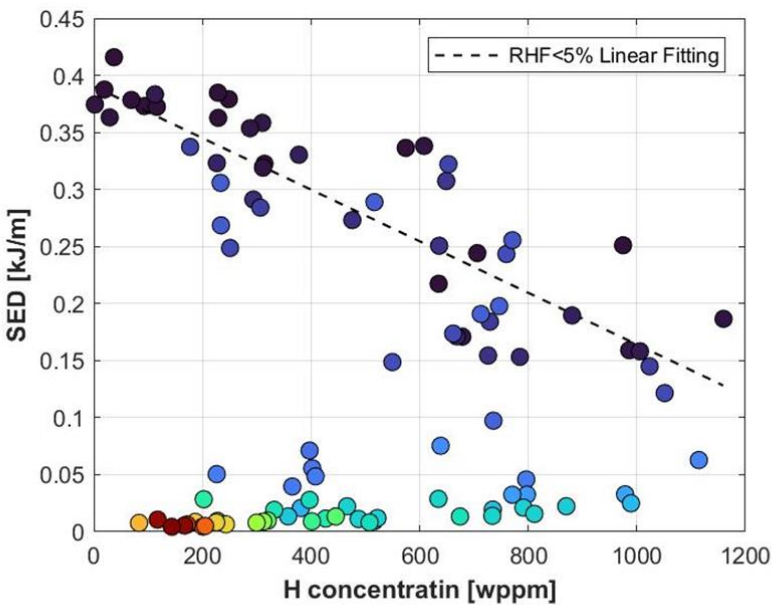

<SED vs. H Concentration>

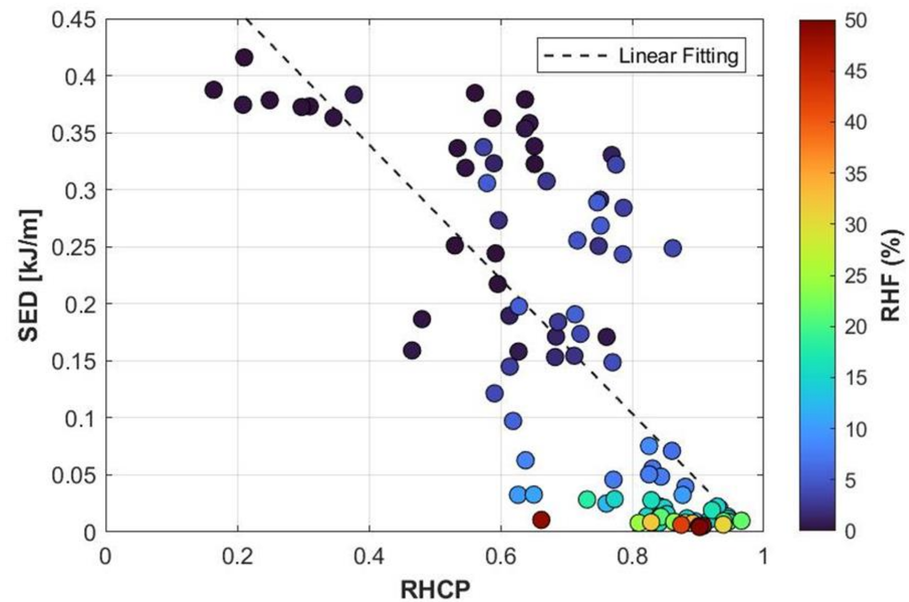

<SED vs. RHCP>

- For RHF < 5% , H concentration plays a predominant role in determining SED.
- RHCP alone presents limited accuracy in predicting SED.

Maximum radial hydride length is another powerful metric

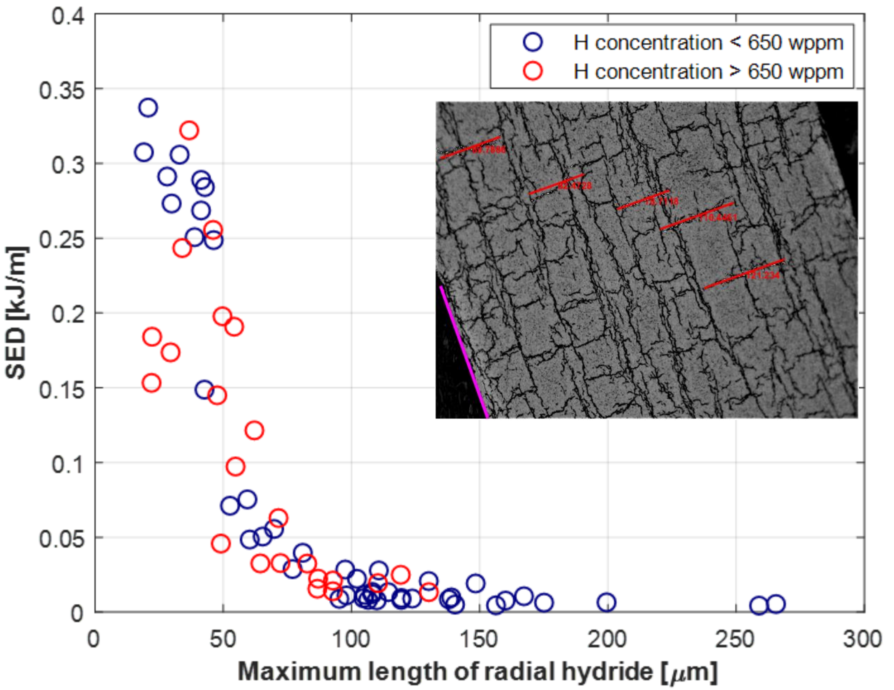

<SED vs. Max radial hydride length>

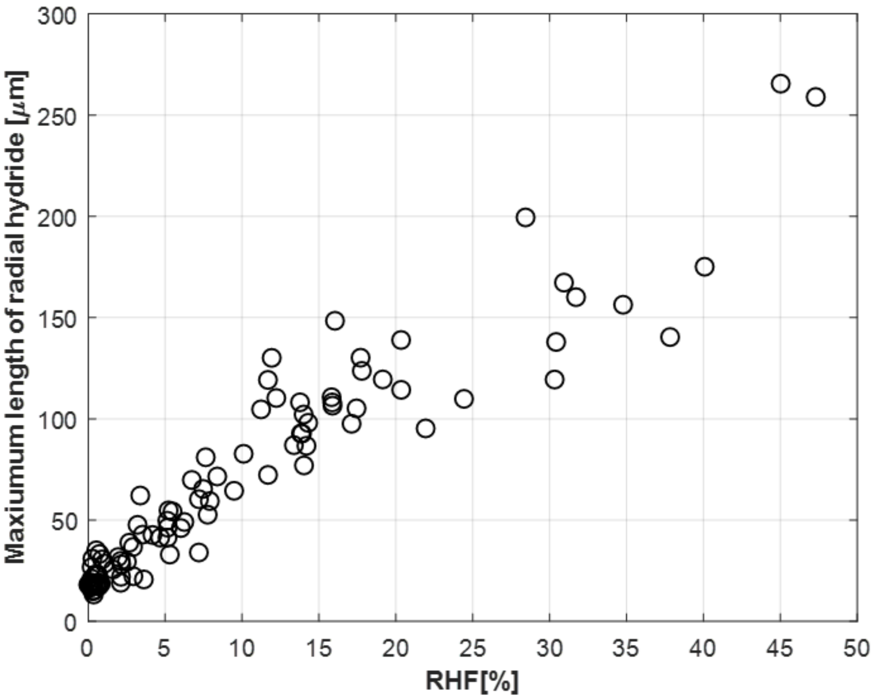

< Max radial hydride length vs. RHF>

- Exhibiting a notable correlation with RHF, maximum radial hydride presents a strong correlation with SED. This is consistent with the principle of fracture mechanics which states that the brittle fracture occurs by a critical flaw.

결론

- **국산 정상운전 성능해석 코드 GIFT**
  - OECD/NEA Data Bank 핵연료 실험 데이터와 검증작업 진행 중
  - 코드 공개예정
- **재료 이미지 분석을 통한 물성변화 예측 방법론**
  - 지르코늄 합금 수소화물 취성분석 적용가능성 확인
  - 다양한 원자력 구조재료 열화현상 (예: 지르코늄 산화, 배관 및 용기 산화)에 적용가능성 있을 것으로 예상
- **핵연료 및 원자력 재료분야 전산 모사의 중요성**

지양해할 차세대 원자로 개발

시스템 성능 혁신 → 신재료 개발 및 테스트 → 인허가 및 현실화 불가능

합리적인 차세대 원자로 개발

가용한 핵연료/구조 재료 → 시스템 성능혁신 → 인허가 및 현실화 가능

시스템 설계와 연계 가능한 핵연료/구조재료 성능해석 코드 중요

Thank you